Analyzing Human Behavior and Memory Activities using Deep Learning for BMI

Author

Khurram Khalil

Regn Number

00000273888

Supervisor

Prof. Dr. Yasar Ayaz

Thesis Co-Supervisor:

Dr. Umer Asgher

DEPARTMENT OF ROBOTICS AND INTELLIGENT MACHINE ENGINEERING
SCHOOL OF MECHANICAL & MANUFACTURING ENGINEERING
NATIONAL UNIVERSITY OF SCIENCES AND TECHNOLOGY
ISLAMABAD
JANUARY 2021

Analyzing Human Behavior and Memory Activities using Deep Learning for BMI

Author

Khurram Khalil

Regn Number

00000273888

A thesis submitted in partial fulfillment of the requirements for the degree of

MS Robotics and Intelligent Machine Engineering

Thesis Supervisor:

Prof. Dr. Yasar Ayaz

Thesis Supervisor's Signature: _____

DEPARTMENT OF ROBOTICS AND INTELLIGENT MACHINE ENGINEERING

SCHOOL OF MECHANICAL & MANUFACTURING ENGINEERING

NATIONAL UNIVERSITY OF SCIENCES AND TECHNOLOGY, ISLAMABAD

JANUARY 2021

Declaration

I certify that this research work titled "*Analyzing Human Behavior and Memory Activities using Deep Learning for BMI"* is my own work. The work has not been presented elsewhere for assessment. The material that has been used from other sources it has been properly acknowledged / referred.

Signature of Student

Khurram Khalil

NUST-SMME-MS-RIME 273888

Plagiarism Certificate (Turnitin Report)

This thesis has been checked for Plagiarism. Turnitin report endorsed by Supervisor is attached.

Signature of Student

Khurram Khalil

Registration Number

00000273888

Signature of Supervisor

Copyright Statement

Acknowledgments

I am thankful to my Creator Allah Subhana-Watala to have guided me throughout this work at every step and for every new thought which You set up in my mind to improve it. Indeed I could have done nothing without Your priceless help and guidance. Whosoever helped me throughout the course of my thesis, whether my parents or any other individual was Your will, so indeed none be worthy of praise but You.

I am profusely thankful to my beloved parents who raised me when I was not capable of walking and continued to support me throughout every department of my life.

I would also like to express special thanks to my supervisor Prof. Yasar Ayaz for his help throughout my thesis and also for Artificial Intelligence and Mobile Robotics and Control courses which he has taught me. I can safely say that I haven't learned any other engineering subject in such depth than the ones which he has taught.

I would also like to pay special thanks to Dr. Umer Asgher for his tremendous support and cooperation. Each time I got stuck in something, he came up with the solution. Without his help, I wouldn't have been able to complete my thesis. I appreciate his patience and guidance throughout the whole thesis.

I would also like to thank Dr. Hasan Sajid, Dr. Muhammad Jawad Khan, and Dr. Umer Asgher for being on my thesis guidance and evaluation committee and express my special thanks to Nabeeha Ehsan for her help. I am also thankful to Mahmoona Khalil and Muhammad Zubair for their support and cooperation.

Finally, I would like to express my gratitude to all the individuals who have rendered valuable assistance to my study.

Dedicated to my exceptional parents and adored siblings whose tremendous support and cooperation led me to this wonderful accomplishment.

Abstract

In the present era, human-machine collaboration is increasing each day with more applications of ergonomics and human factors in industrial and socio-technical environments. This has amplified the need for human factors while designing collaborative applications. Among these macro-human factors; human's mental workload (MWL), stress level, and mental cognitive states are vital to consider while planning system safety and risk assessment. Similarly, Brain-Computer Interface (BCI) provides a means of contact between the human brain and external devices by recognizing the person's intent using brain generated signals and translating them into external commands and is critical for patients suffering from severe motor disabilities. Cognitive brain signals acquired with functional near-infrared spectroscopy (fNIRS) has come out to be a potential non-invasive neuroimaging solution to monitor brain states for said purposes. Conventionally, the Machine Learning (ML) algorithms are used for the classification of brain states from acquired neuroimaging signals. The difficult part in the conventional ML classification algorithms is feature extraction, feature selection, and dimensionality reduction the neuroimaging data. A novel deep learning (DL) framework is proposed, which utilizes a convolutional neural network (CNN) and recurrent neural network (RNN) variant namely Long Short-Term Memory (LSTM) that solved the feature engineering challenges. However, bypassing the challenges of feature engineering through DL techniques comes at the cost of long training time, the computational complexity of the system, and the requirement for an enormous amount of data for training. The computational complexity of ML and DL algorithms is measured and the appropriate algorithms are suggested in different use cases. The symmetric homogenous instance-based transfer learning method is applied to CNN to solve the complex training time, big data requirement, and calibration time of BCI systems.

Key Words: *BCI, fNIRS, ML, DL, Long Short Term Memory (LSTM), Transfer Learning*

Table of Contents

List of Figures

List of Tables

CHAPTER 1: INTRODUCTION

The research work in this dissertation has been presented in multiple parts. The first part is related to the detailed analysis of Human behavior and memory activities in the brain using different machine learning (ML) and deep learning (DL) classification algorithms. The next part includes the comparison between the computational requirement of different ML and DL algorithms for analyzing human behavior and memory activities in the brain for a brain-machine interface. Further in the line, the fast and efficient heartbeat classification algorithm is presented, and then the novel application of mental workload in soft exoskeleton (servo motor driven) fNIRS-based brain-computer interface (BCI) system is discussed. Lastly, the novel symmetric based homogenous transfer learning is applied on fNIRS data to reduce calibration and training time.

1.1 Literature Review

Neuroergonomics is a relatively new field that focuses on the evaluation of the brain responses generated as a result of uncontrolled human behaviors such as physiology, feelings, intellect, decisions, and perceptions [1]–[4]. Passive BCI is among one of the important sub research topics of neuroergonomics. A passive BCI is usually designed using uncontrolled and subjective brain signals to translate uncontrolled user intentions into external commmads [2]. Among all these passive brain activities the one activity that stands out is mental-workload (MWL). Mental workload (MWL) is a most complex and intricate that consists of perception, neurophysiologic processes, (STM & LTM), and cognitive functions, neurophysiologic processes [5]. The reason behind irrational decision-making is MWL that further leads to safety hazards [6]. For instant 3.9% and 33% of the cause of traffic accidents in the United States and New Zealand is drowsiness that is one of the passive brain activities [7]. In the current empire of human-machine interaction, contemporary and innovative technology need yet more mental requirements for consumers and workers in order to ensure safety, protection, and profit maximization [8]. There are several approaches for MWL estimation; the most common or popular techniques are performance, subjective rating, and physiological measures. Two metrics that are used to track the record of a person's progress are 1) accuracy and, 2) reaction time is used by the performance rating method. On the other hand, questioners are being devised by

surveyors to evaluate the emotional and mental conditions of the substance used by subjective rating methods. To measure the MWL during the experimentation, self-reporting and thoughts of the subject matter are judged. Numerous kinds of research utilize tests such as the National Aeronautics and Space Administration's Task Load Index (NASA-TLX) in order to calculate or measure the cognitive load [9]. Another example of such a test is the SWAT. The subjective technique is the self-reporting procedure that is dependent on the judgment of the respondent, that again may be influenced by unfairness, low enthusiasm, lapses in understanding natural environment changes, and uncertainty; that is a major limitation of this method [10]. Other reasons include these aforementioned methods may not be able to consider the different types of physical efforts related to activities involving the movement of arms, feet, and other periphery muscles or the entire physique of a person [11]. While the physiological procedures provide a real-time evaluation and need a tinier sample size and higher viability to approximate stable cognitive mental workload states [12]. The different physiological sensors, such as fMRI, EEG, eye response measurement, HRV, and fNIRS are most widely used for the examination of the mental workload. Based on portability, low cost, and non-invasiveness, electroencephalography (EEG) and fNIRS are the two for the most part widely used modalities for the rehabilitation of a patient [13], [14]. In comparison to EEG, fNIRS has better spatial resolution while EEG has better temporal resolution [15]–[17]. BCI based applications are now getting popular and become more useful and powerful. A BCI system mainly consists of four essential components namely signal processing, feature extraction, classification, and command generation. Among these parts, Signal processing and feature extraction are the most important ones. Over the years, EEG was used as a default device for BCI purposes. Recently, the use of fNIRS is becoming popular to utilize the cognitive states of a person for BCI applications.

The BCI provides a method of communication between the human brain and the external devices through signals generated from the brain without the involvement of the peripheral nervous system [18]. BCI is among such neurofeedback methods that can enhance the condition of life of patients suffering from serious motor debilities due to tetraplegia, stroke, ad other spinal cord injuries [19]. BCI has also applications in neuro-rehabilitation, communication and control, motor therapy and recovery, brain monitoring, and neuro-ergonomics [4][20][21]. The major non-invasive BCI modalities include fMRI, EEG, MEG, and fNIRS. Among these non-invasive BCI modalities, EEG, and fNIRS are the foremost modalities in terms of price and

manageability [17][22]. EEG measures brain activity by calculating the voltage fluctuations from neurons' action potentials while fNIRS detects the brain activity concerning the changes in hemodynamic response [23][24].

To use BCI out of the laboratory on daily basis, BCI needs to address several challenges such as robust signal acquisition, extracting valuable knowledge from the acquired raw brain signals (either electrical or hemodynamic) for control-command generation, etc [25][26]. Another main problem is the requirement of recalibrating the BCI system. The recalibration requirement is required for every new session and subject. Usually, the calibration time for electroencephalography (EEG) and functional Near-Infrared spectroscopy (fNIRS) based BCI systems may take up to 20 minutes to 30 minutes, depending upon the situations, for each new session [27][28]. This is a strenuous and exhausting total of time that the subjects and patient have to undertake before the BCI system is completely practical again. Also, another reason for having a such lengthy calibration time for neuroimaging-based BCI is due to the high dimensionality of EEG and fNIRS signals that have a very low signal-to-noise ratio (SNR) [29]. To successfully classify the correct brain states, "obtained neuroimaging signals are usually handled in the four stages namely: preprocessing, feature extraction, classification, and command generation" [30][31]. The extracted features from brain signals are used to train the classifier. The collection of neuroimaging data is very complicated and also expensive both in terms of time and cost that makes it very hard to develop a substantial-scale, high-quality marked dataset for the training of deep learning models. That results in limited trials available for training. From low SNR signals, it is extremely difficult to approximate probability distributions of the features, usually in the case of machine learning algorithms. Another important factor is the non-stationary nature of fNIRS and EEG signals. The exact brain state depends on different reasons such as the mental and psychological states, concentration level, drowsiness and fatigue, anatomical differences between subjects, and statistical variations in the data [32][33]. The instrumental noise and experimental error such as changes in the impedance of the electrodes due to sweating may also temper the acquired brain signals [34]. All these facts combine results in the trained classifier performing poorly on new session data. The different studies tried to address these challenges by exploiting different methods and algorithms while trying to keep the models' accuracy in an acceptable range [28][35][36][37]. Transfer learning might be an encouraging method to deal with the above problem.

1.2 Motivation

Mental workload (MWL) is one of the key scopes of Neuroergonomics necessary to consider while planning for industrial processes and systems [6]. MWL is itself a complex function involving multiple intra-cognitive processes at a time including the perception of the environment, neurophysiology of the brain, short term memory, long term memory, and different cognition functions happening at the time of activity. "MWL is a key focus with the advancement in the field of Human-Machine Interaction (HMI) as all levels of organization from operators up to the top management demand greater cognition from their workers" [8]. Different researches have been carried on MWL measurement and analysis using different methods mainly including physiological or performance measures, and subjective rating. Subjective Workload Analysis (SWAT) and NASA's Task Load Index (TLX) used subjective rating methods to measure MWL involving self-reporting mechanisms and questioners from subjects. While performance measures include methods like the accuracy of a response and reaction time metrics to measure the MWL of subjects. Feelings and motivation of respondents involved at the time of the experiment produce biased results making these methods less reliable and more prone to errors and mistakes [38]. Secondly, another major drawback of these methods is they do not involve any physical work while assessment of MWL which is an essential requirement for accurate measurement [11].

Over the years, the most commonly followed paradigm is to detect the imagined body kinematics using neuro-imaging modalities and decode them using the regression model, and then mapped them on a social robot. Abiri et. al. [39] presented a work in which the scalp EEG was recorded in which the user was imagining different body kinematics while [40] has presented different communication types available in BCI. Ortiz et al. and Volosyak et al. [41], [42] have presented a review of non-invasive EEG signal processing techniques for SSVEP based applications, and [43] has presented a comprehensive study of different useful features in fNIRS-EEG based activities. Similarly, [17], [29] discussed different machine learning and deep learning techniques formally used in fNIRS and hybrid applications. Erkan et al. [44], has reported that minimum energy combination (MEC) and canonical correlation analysis (CCA) can be used in the detection of SSVEP signals in EEG recording but MEC is recommended for synchronous SSVEP stimulus. Gao. et al. [45] showed the feasibility of the SSVEP using an electric apparatus. The patient is introduced to different flickering lights (boxes) which flashes at

different rates and represents different actions against each (chosen from a menu). It is not necessary that the environment, where the SSVEP signals are being taken, is fully calm or it might possible that the person, using SSVEP, is not fully calm. Chaudhary et al. [40] have studied the effect of deliberately introduced perturbations while using SSVEP. Introduced perturbations were speaking, listening, and thinking while EEG is being recorded. Results showed that speaking and thinking affect the classification accuracy while listening does not affect much. In [46]–[48] authors recorded fNIRS recordings for measurement of emotions and cognitive processing from the prefrontal cortex (PFC) region. Different studies have used fNIRS to detect motor imagery and mental arithmetic tasks [17], [49]. Multiple types of noise are present in fNIRS and EEG including different artifacts as well. Xie. et al. [50] has studied the effect of spatiotemporal visual noise on the compensation of mental load and fatigue and [51] has given the inclusion of fuzzy control in this field.

Cardiovascular disease (CD) describes the class of illnesses that include the heart problems such as narrowed and/or completely blocked human blood vessels [52]. Cardiovascular disease is frequently used interchangeably with the terms such as heart diseases or heart illnesses. According to the US DHHS (Department of Health and Human Services), cardiovascular diseases are the foremost cause of death for both men and women [53]. The important notes and facts released by the WHO (World Health Organization) in the year 2017 state that an estimated 17.9 million died from cardiovascular diseases in 2016. This alone counts as the highest cause of death worldwide. The various obsessive symptoms of cardiovascular systems can be examined by heart-related signals such as heart electrical signals and heart sound signals. The electronic activity of the heart is measured by electrocardiographs (ECG) and sound signals are measured by phonocardiograms (PCG) [54]. Nevertheless, the actual and accurate manual assessment of ECG signals auscultation alters the skills and different personal skills of the physicians which are obtained from a long medical experience [55]. Traditional ML classification algorithms such as SVM, LDA, and k-NN rely deeply on the effectiveness and classifiable information of mined features also known as manual feature engineering. Although extracted features, representing statistical summarization of raw ECG signal, provide us with the satisfactory and acceptable representation of the heart electrical signal, the very recent deep learning-based automated feature extraction such as convolutional neural networks, etc, and

representation methods have end-to-end learning competence and are proficient of forecasting with reasonably high accuracy [54][56].

Transfer learning is a method that is used to enhance the accuracy of a classification algorithm trained from the target domain and transferring common information to the target domain [57]. Transfer learning is mostly used in situations when there might be a limited amount of training annotated data with supervised samples from the original or target domain. Transfer learning successfully experiments in different machine learning and deep learning applications such as natural language processing, image recognition, image segmentation, pose estimation, and video captioning. Transfer learning all in all is quite a new field for BCI and it is slowly gaining researchers' interest all over the globe. Transfer learning describes: "the procedure of using data recorded in one task to boost performance in another, related task (for a more exhaustive review of the machine learning literature, see [58]), as such, long sessions of BCI usage present unique problems in terms of consistent classification" [59][18].

1.3 Novelty

I presented an extreme learning machine (ELM) based ECG classification algorithm. The strength of this newly proposed classifier remains in its intrinsic fast and inexpensive algorithm that does not require backpropagation for the training. In the next study, I applied a fairly new class of deep learning algorithms i.e. CNN on hemodynamic concentration changes brain signals acquired through the fNIRS device. The results of a convolutional neural network are compared with that of a machine learning algorithm (SVM). The findings suggest that the convolutional neural network outperformed the support vector machine with a huge margin. The four-phase Mental Workload (MWL) was evaluated and classified using machine learning (SVM, k-NN, ANN) and deep learning (CNN and LSTM) algorithms using the fNIRS dataset. Targeting the most affected patients of stroke, I devised two commands fNIRS based servo tendon driven exoskeleton hand for grasping task. The two-level of the mental workload are recorded with the fNIRS device at 8 Hz sampling frequency. The maximum accuracy attained is 91.31% while the minimum averaged accuracy is 80.15%. Targeted channels are PF1, PF2, and PFz. After normalizing channel readings, we used the 4^{th} order low-passed Butterworth bandpass to remove high-frequency artifacts due to breathing, blood pressure, and heartbeat. Then we used SVM to generate a command (either open or close) for a prosthetic hand. Results showed the

effectiveness of the used technique for those suffering from a severe level of strokes. I explored the feature-based transfer learning approach for the classification domain to reduce the training time and calibration time for the fNIRS-based BCI systems. In the first approach, we used 16 subjects to train the CNN network, namely learned CNN network, and learn the source domain knowledge of the n-back dataset. Further, we split the remaining 10 subjects into two groups i.e control and baseline. We then train the control group with the learned CNN network and baseline with randomly initialized CNN network and compared their accuracies using statistical analysis. The results suggested that applying the proposed feature-based transfer learning algorithms could lead to achieving the maximum saturated accuracy 20 epochs sooner than the baseline group which in turn reduces the training time. The proposed transfer learning method also outperformed the averaged accuracy achieved using the learned CNN model over the traditional CNN model by 12%. In the second experiment, we proved that instance-based transfer learning can significantly reduce the calibration time with reasonable accuracy on the 10:90 train-test ratio and become saturate on the 30:70 train-test split ratio of the dataset. In the next study, resource and classification capabilities of machine learning (LDA, k-NN, and SVM) and deep learning (ANN, CNN, and LSTM) algorithms are computed on fNIRS data acquired from 26 subjects performing mental workload activities. The theoretical computation complexities of ML and DL algorithms are computed and compared the practical processing time, train - test time complexity, and resource requirements. The finding suggests that in terms of time requirements, the machine learning algorithms are the fastest. Within machine learning algorithms, LDA is the least compute-intensive algorithm while SVM and k-NN depend on the applied kernel and numbers of training samples, respectively. However, the downside of machine learning algorithms is their accuracy and generalizability decrease with an increase in classification commands, in addition to the fact that they mostly rely on handcrafted feature extraction and require domain knowledge. Among deep learning algorithms, the time complexity of ANN and CNN is comparable but in terms of the accuracy alone, the ANN entirely depends upon the handcrafted features while CNN has impressive self-feature extraction. The recurrent neural network (RNN) has shown impressive accuracies as compared to the rest of the algorithms. On the other hand, RNNs are compute-intensive in terms of train-test time and not be feasible for real-time BCI applications. The RNN variant, LSTM is also analyzed in this study and concluded as a better choice for the offline brain signal analysis. Meanwhile, CNN offers an optimal

compromise between the accuracy and time requirement. Machine learning algorithms are still recommended for real-time applications primarily designed to work without any delay.

1.4 Structure of Research

The rest of the manuscript is devised as follows: Chapter 2 explains the existing theory and also appends the proposed theory, in Chapters 3 the viability of deep learning for BCI is proved as a concept and then different advanced deep learning algorithms are applied on the fNIRS data. Chapter 4 compares the machine learning vis-à-vis deep learning in terms of computation complexity for pre-processing time, training time, and test time. In chapter 5 the downsides of deep learning algorithms for BCI are discussed and a novel symmetric homogenous transfer learning framework is proposed to combat those downsides. In chapter 6 a soft-exoskeleton mental workload based fNIRS solution is presented for patients suffering from motor disabilities. In chapter 7 conclusion is drawn and different pathways for future research are suggested. In the end, references are given.

CHAPTER 2: THEORY OF RESEARCH

2.1 Existing Theory

The use of direct communication between the brain and computer machines is becoming popular in the realm of neuroscience. Such techniques are becoming indispensable element for individuals who are unable to generate mechanical control commands due to neuromuscular disorder, the consequence of stroke, Locked-in syndrome (LIS), spinal injuries, or Amyotrophic lateral sclerosis (ALS) [60][61]. Aside from the medical application, the use of brain activities as a means of communication spans on brain-computer interface (BCI), neurofeedback, neuro-ergonomics, human-human, and human-machine interaction, and ultimately brain to brain interface fields [62][63]. The best available approach to record brain activities without carrying risks associated with surgery and avoiding ethical issues is with non-invasive neuroimaging modalities [41][64]. Non-invasive neuroimaging modalities include electroencephalography (EEG), functional magnetic resonance imaging (fMRI), electrooculography (EOG), magnetoencephalography (MEG), and functional near-infrared spectroscopy (fNIRS) [29][43].

Each neuroimaging modality has its pros and cons. The main factors, however, deciding effective use of neuroimaging modality are usually cost of the equipment, portability, and required spatial and temporal resolution for the problem at hand. Neuroimaging modalities may use together in hybrid settings to enhance accuracy, increase control command or decrease detection time of brain signals [65][66][67]. Among hybrid neuroimaging modalities, EEG and fNIRS are low cost, portable, and can be applied in non-laboratory settings. EEG measures voltage fluctuations in the brain due to cortical postsynaptic current variations in neurons [68]. Several electrodes are placed on the scalp to measure EEG signals. It has a better temporal resolution (≈ 0.05 s). It can measure cortical activity in milliseconds by taking thousands of brain snapshots, but it struggles in spatial resolution (≈ 10 mm) [69]. While fNIRS measures blood oxygen level-dependent (BOLD) response using near-infrared (NIR) light to construct a functional brain neuroimage. fNIRS, like EEG, is portable, low cost, and easier to use. It is less prone to electrical noises and has a better spatial resolution than EEG that is affected up to a few centimeters [29]. Theoretically, EEG and fNIRS should coverup each-other weaknesses and endow better, information-rich, and in-depth neuroimaging details. EEG and fNIRS combination

in hybrid mode is thought to be a significant breakthrough [4]. However, in practice, fNIRS measurements suffer from the inherent delay due to the nature of the hemodynamic response, which conduces slow command generation [70]. Also, there is a vast difference in the sampling rate of both devices. Different workarounds are used to compensate for the delayed fNIRS response. The time lag can be significantly decreased for hybrid EEG-fNIRS modalities by detecting initial dip (i.e., the phenomenon that HBO drops and HbR increases with neural firing) instead of hemodynamics [71], [72]. Another technique is to reinforce EEG data generated commands with fNIRS data, e.g. remove false positive alarms using fNIRS data in the commands that are made through EEG data. The EEG data acquisition rate is 10-100 times more than that of fNIRS. In hybrid settings, the most common opted practice is to downsample EEG readings to make them compatible with fNIRS low sampling rate. A lot of valuable information is also lost with the discarded data [117]. Acquired fNIRS raw signals suffered from instrumental, experimental, and physiological noises. Instrument noises are due to hardware and surrounding environment and usually in the form of high frequencies and can be removed by a low-pass filter. Experimental errors may be caused due to different motion artifacts such as head movement slippage of optodes on hairs or due to sudden light intensity change. The motion artifacts are removed using Wiener filtering-based methods [25], Savitzky-Golay filter [73], Wavelet-analysis-based methods [74], etc.

Similarly, physiological noises (caused due to heartbeat, respiration, Mayer waves, etc.) are removed using different techniques in the literature. The most common of them are bandpass filtering, principal component analysis, independent component analysis, adaptive filtering, statistical parametric mapping. Removing all these noises cut a reasonable chunk of raw data, and cleaned data is even smaller in size than the original. Now down sampling EEG signal to match fNIRS pre-processed data results in huge data loss and potentially result in loss of brain activity information. Conventionally, statistical, and machine learning algorithms were used to discriminate between brain signals that were not adequately capable of learning sophisticated features anyway and may tolerate that discarded data. With the recent advancement in artificial intelligence, the application of powerful, more intelligent, and data-hungry deep learning algorithms is increasing. The Convolutional Neural Network (CNN) is one of the deep learning algorithms that have achieved the state of the art results on vision and speech recognition and got considerable attention within the BCI field (3, 4 papers). The strength of CNN lies in the fact that

it does not require handcrafted features. The feature extraction and classification are unified and learned jointly.

The BCI provides a method of communication between the human brain and the external devices through signals generated from the brain without the involvement of the peripheral nervous system [18]. BCI is among such neurofeedback methods that can improve the quality of life of patients suffering from severe motor disabilities due to tetraplegia, stroke, ad other spinal cord injuries [19]. BCI has also applications in neuro-rehabilitation, communication and control, motor therapy and recovery, brain monitoring, and neuro-ergonomics [4][20][21]. The major non-invasive BCI modalities include fMRI, EEG, MEG, and fNIRS. Among these non-invasive BCI modalities, EEG, and fNIRS are the foremost modalities in terms of price and manageability [17][22]. EEG measures brain activity by calculating the voltage fluctuations from neurons' action potentials while fNIRS detects the brain activity concerning the changes in hemodynamic response [23][24]. fNIRS headset P-fNIRSSyst is used, which the patient uses on the PFC scalp, for the data acquisition. The P-fNIRSSyst is a continuous wave fNIRS system that consists of 12 channels arranged in arrays like structure, integrated with 3 near-infrared sources (NIR) having a dual-wavelength of 760 nm and 850 nm and 8 photodetectors. The sampling rate of P-fNIRSSyst is 8 Hz. The fNIRS system estimates the neuronal activity of the brain by measuring hemodynamic concentration changes in the PFC in the form of oxygenated (HbO) and deoxygenated hemoglobin (HbR). The acquired brain hemodynamic concentration changes (ΔHbO and HbR) are then used to generate commands for BCI systems. The complete architecture and system structural design are shown in Figure 8. The subject with the robotic hand wears the fNIRS device on the scalp which is continuously measuring hemodynamic concentration changes in the prefrontal cortex as shown in Figure.

Over the years, the most commonly followed paradigm is to detect the imagined body kinematics using neuro-imaging modalities and decode them using the regression model, and then mapped them on a social robot. Abiri et. al. [39] presented a work in which the scalp EEG was recorded in which the user was imagining different body kinematics while [40] has presented different communication types available in BCI. Ortiz et al. and Volosyak et al. [41], [42] have presented a review of non-invasive EEG signal processing techniques for SSVEP based applications, and [43] has presented a comprehensive study of different useful features in fNIRS-EEG based activities. Similarly, [17], [29] discussed different machine learning and deep

learning techniques formally used in fNIRS and hybrid applications. Erkan et al. [44], has reported that minimum energy combination (MEC) and canonical correlation analysis (CCA) can be used in the detection of SSVEP signals in EEG recording but MEC is recommended for synchronous SSVEP stimulus. Gao. et al. [45] showed the feasibility of the SSVEP using an electric apparatus. The patient is introduced to different flickering lights (boxes) which flashes at different rates and represents different actions against each (chosen from a menu). It is not necessary that the environment, where the SSVEP signals are being taken, is fully calm or it might possible that the person, using SSVEP, is not fully calm. Chaudhary et al. [40] have studied the effect of deliberately introduced perturbations while using SSVEP. Introduced perturbations were speaking, listening, and thinking while EEG is being recorded. Results showed that speaking and thinking affect the classification accuracy while listening does not affect much. In [46]–[48] authors recorded fNIRS recordings for measurement of emotions and cognitive processing from the prefrontal cortex (PFC) region. Different studies have used fNIRS to detect motor imagery and mental arithmetic tasks [17], [49]. Multiple types of noise are present in fNIRS and EEG including different artifacts as well. Xie. et al. [50] has studied the effect of spatiotemporal visual noise on the compensation of mental load and fatigue and [51] has given the inclusion of fuzzy control in this field.

The results suggested that applying the proposed feature-based transfer learning algorithms could lead to achieving the maximum saturated accuracy 20 epochs sooner than the baseline group which in turn reduces the training time. The proposed transfer learning method also outperformed the averaged accuracy achieved using the learned CNN model over the traditional CNN model by 12%. In the second experiment, we proved that instance-based transfer learning can significantly reduce the calibration time with reasonable accuracy on the 10:90 train-test ratio and become saturate on the 30:70 train-test split ratio of the dataset. In the next study, resource and classification capabilities of machine learning (LDA, k-NN, and SVM) and deep learning (ANN, CNN, and LSTM) algorithms are computed on fNIRS data acquired from 26 subjects performing mental workload activities. The theoretical computation complexities of ML and DL algorithms are computed and compared the practical processing time, train - test time complexity, and resource requirements. The finding suggests that in terms of time requirements, the machine learning algorithms are the fastest. Within machine learning algorithms, LDA is the least compute-intensive algorithm while SVM and k-NN depend on the applied kernel and

numbers of training samples, respectively. However, the downside of machine learning algorithms is their accuracy and generalizability decrease with an increase in classification commands, in addition to the fact that they mostly rely on handcrafted feature extraction and require domain knowledge. Among deep learning algorithms, the time complexity of ANN and CNN is comparable but in terms of the accuracy alone, the ANN entirely depends upon the handcrafted features while CNN has impressive self-feature extraction. The recurrent neural network (RNN) has shown impressive accuracies as compared to the rest of the algorithms. On the other hand, RNNs are compute-intensive in terms of train-test time and not be feasible for real-time BCI applications. The RNN variant, LSTM is also analyzed in this study and concluded as a better choice for the offline brain signal analysis. Meanwhile, CNN offers an optimal compromise between the accuracy and time requirement. Machine learning algorithms are still recommended for real-time applications primarily designed to work without any delay.

2.2 Proposed Theory

Over the years, the most commonly followed paradigm is to detect the imagined body kinematics using neuro-imaging modalities and decode them using the regression model, and then mapped them on a social robot. Abiri et. al. [39] presented a work in which the scalp EEG was recorded in which the user was imagining different body kinematics while [40] has presented different communication types available in BCI. Ortiz et al. and Volosyak et al. [41], [42] have presented a review of non-invasive EEG signal processing techniques for SSVEP based applications, and [43] has presented a comprehensive study of different useful features in fNIRS-EEG based activities. Similarly, [17], [29] discussed different machine learning and deep learning techniques formally used in fNIRS and hybrid applications. Erkan et al. [44], has reported that minimum energy combination (MEC) and canonical correlation analysis (CCA) can be used in the detection of SSVEP signals in EEG recording but MEC is recommended for synchronous SSVEP stimulus. Gao. et al. [45] showed the feasibility of the SSVEP using an electric apparatus. The patient is introduced to different flickering lights (boxes) which flashes at different rates and represents different actions against each (chosen from a menu). It is not necessary that the environment, where the SSVEP signals are being taken, is fully calm or it might possible that the person, using SSVEP, is not fully calm. Chaudhary et al. [40] have studied the effect of deliberately introduced perturbations while using SSVEP. Introduced

perturbations were speaking, listening, and thinking while EEG is being recorded. Results showed that speaking and thinking affect the classification accuracy while listening does not affect much. In [46]–[48] authors recorded fNIRS recordings for measurement of emotions and cognitive processing from the prefrontal cortex (PFC) region. Different studies have used fNIRS to detect motor imagery and mental arithmetic tasks [17], [49]. Multiple types of noise are present in fNIRS and EEG including different artifacts as well. Xie. et al. [50] has studied the effect of spatiotemporal visual noise on the compensation of mental load and fatigue and [51] has given the inclusion of fuzzy control in this field. I presented an extreme learning machine (ELM) based ECG classification algorithm. The strength of this newly proposed classifier remains in its intrinsic fast and inexpensive algorithm that does not require backpropagation for the training. In the next study, I applied a fairly new class of deep learning algorithms i.e. CNN on hemodynamic concentration changes brain signals acquired through the fNIRS device. The results of a convolutional neural network are compared with that of a machine learning algorithm (SVM). The findings suggest that the convolutional neural network outperformed the support vector machine with a huge margin. The four-phase Mental Workload (MWL) was evaluated and classified using machine learning (SVM, k-NN, ANN) and deep learning (CNN and LSTM) algorithms using the fNIRS dataset. Targeting the most affected patients of stroke, I devised two commands fNIRS based servo tendon driven exoskeleton hand for grasping task. The two-level of the mental workload are recorded with the fNIRS device at 8 Hz sampling frequency. The maximum accuracy attained is 91.31% while the minimum averaged accuracy is 80.15%. Targeted channels are PF1, PF2, and PFz. After normalizing channel readings, we used the 4^{th} order low-passed Butterworth bandpass to remove high-frequency artifacts due to breathing, blood pressure, and heartbeat. Then we used SVM to generate a command (either open or close) for a prosthetic hand. Results showed the effectiveness of the used technique for those suffering from a severe level of strokes. I explored the feature-based transfer learning approach for the classification domain to reduce the training time and calibration time for the fNIRS-based BCI systems. In the first approach, we used 16 subjects to train the CNN network, namely learned CNN network, and learn the source domain knowledge of the n-back dataset. Further, we split the remaining 10 subjects into two groups i.e control and baseline. We then train the control group with the learned CNN network and baseline with randomly initialized CNN network and compared their accuracies using statistical analysis. The results suggested that applying the

proposed feature-based transfer learning algorithms could lead to achieving the maximum saturated accuracy 20 epochs sooner than the baseline group which in turn reduces the training time. The proposed transfer learning method also outperformed the averaged accuracy achieved using the learned CNN model over the traditional CNN model by 12%. In the second experiment, we proved that instance-based transfer learning can significantly reduce the calibration time with reasonable accuracy on the 10:90 train-test ratio and become saturate on the 30:70 train-test split ratio of the dataset. In the next study, resource and classification capabilities of machine learning (LDA, k-NN, and SVM) and deep learning (ANN, CNN, and LSTM) algorithms are computed on fNIRS data acquired from 26 subjects performing mental workload activities. The theoretical computation complexities of ML and DL algorithms are computed and compared the practical processing time, train - test time complexity, and resource requirements. The finding suggests that in terms of time requirements, the machine learning algorithms are the fastest. Within machine learning algorithms, LDA is the least compute-intensive algorithm while SVM and k-NN depend on the applied kernel and numbers of training samples, respectively. However, the downside of machine learning algorithms is their accuracy and generalizability decrease with an increase in classification commands, in addition to the fact that they mostly rely on handcrafted feature extraction and require domain knowledge. Among deep learning algorithms, the time complexity of ANN and CNN is comparable but in terms of the accuracy alone, the ANN entirely depends upon the handcrafted features while CNN has impressive self-feature extraction. The recurrent neural network (RNN) has shown impressive accuracies as compared to the rest of the algorithms. On the other hand, RNNs are compute-intensive in terms of train-test time and not be feasible for real-time BCI applications. The RNN variant, LSTM is also analyzed in this study and concluded as a better choice for the offline brain signal analysis. Meanwhile, CNN offers an optimal compromise between the accuracy and time requirement. Machine learning algorithms are still recommended for real-time applications primarily designed to work without any delay.

CHAPTER 3: ANALYSIS OF DIFFERENT BRAIN ACTIVITIES USING MACHINE LEARNING AND DEEP LEARNING

The four-level MWL with varying difficulty level data is acquired using fNIRS from fifteen healthy subjects. The high-frequency artifacts and other physiological noises are eliminated using a 4th-order Butterworth low-frequency bandpass filter. The statistical significance of the acquired fNIRS data is verified using student p and t-test. The three conventional machine learning classifiers namely Support Vector Machine, k-NN, and Artificial Neural Networks alongside two deep learning algorithms namely Convolutional Neural Network and LSTM are used for four-level MWL discrimination and classification. However, the main contribution of this research is as follows: (1) To the best of the authors' knowledge, for the first time this study has applied LSTM on fNIRS time series data for four class MWL segregation and its comparison with Convolutional Neural Network. (2) Machine Learning classifiers outperformed by a heavy margin as compared with the DL classifiers and within the deep learning algorithms, the LSTM presents considerably improved classification accuracy as compared to Convolutional Neural Network. The used fNIRS device has 12 channels operating on two wavelengths of 760 nm and 850 nm with a continuous-wave (CW) system namely "P-fNIRSSyst" [117]. This device is used to measure hemodynamic concentration changes from the prefrontal cortex area of the brain [75]. The data acquisition rate is set to the 8 Hz (each channel per second), which essentially converts into 192 samples per channel. The fNIRS channel configuration is according to Fig. 2. The most common features that can be used for machine learning classifiers are explained below:

Feature eNGINEERING

Mean: In statistics, arithmetic mean is a single value referring to the central tendency of given data. It is determined by the sum of all the data points of a data over the total number of data points. Mathematically it is expressed as:

$$\mu = \frac{1}{n}\sum_{i=1}^{n} x_i$$

Where x refers to the data points of a given data set from 1 to n.

Median: Median is another statistical number to refer to the central tendency of the data. It is determined by arranging the data in ascending or descending order and then finding the central data point. Mathematically it is expressed as:

$$Median = (\frac{n+1}{2})\ th\ data\ point$$

When the number of data points is odd. Where n refers to the number of data points. While, in the case when the number of data points is even, the median is:

$$Median = \frac{1}{2}\ [\frac{n}{2} + (\frac{n}{2} + 1\ )]\ th\ data\ points$$

Mode: In statistics, the mode of a data set is the value repeated most often.

Standard deviation: Standard deviation, in statistics, is used to quantify the dispersion of data points within a distribution from a mean value. Mathematically it is expressed as:

$$\sigma = \sqrt{\frac{1}{n-1}\sum_{i=1}^{n}(x_i - \mu)^2}$$

Where x refers to the data points from 1 to n, n refers to the total number of data points and μ is the arithmetic mean of the data set.

Variance: Variance is defined as the squared standard deviation and used to quantify the deviation of data points of a distribution from the mean value. Mathematically variance is expressed as:

$$\sigma^2 = \frac{1}{n-1}\sum_{i=1}^{n}(x_i - \mu)^2$$

Minima: In mathematical analysis, minima refer to the smallest value of a function or distribution. Symbolically it is written as:

$$x_0 \in \text{ X is minima of a function}$$

Where f: X → R if (□x ∈ X) f (x_0) ≤ f (x)

Maxima: Maxima, in mathematical analysis, is referred to as the largest value of a data point within a given range or distribution. Symbolically it is written as:

$$x_0 \in \text{ X is the maxima of a function}$$

Where f: X → R if (□x ∈ X) f (x_0) ≥ f (x)

Slope: In mathematics, the slope or gradient of a line is a value referring to both the steepness and the direction of the line. It is the ratio of the vertical difference to the horizontal difference between two distinct points on a line and thus mathematically expressed as:

$$m = \frac{\Delta y}{\Delta x}$$

Where, Δy and Δx, are the vertical difference and horizontal difference between two points on a line respectively.

Kurtosis: In statistical analysis, kurtosis is the measure of a peak around the mean distribution. Mathematically it is expressed as:

$$Kurtosis = \frac{\sum_{i=1}^{n} \frac{(x_i - \mu)^4}{n}}{\sigma^4}$$

Where, x_i are the data points of the distribution, μ is the mean, σ is the standard deviation of the distribution. While n is the sample size.

Skewness: In statistics, skewness is the measure of the asymmetry of a distribution about its mean. It can be positive, negative, or undefined. Mathematically it is defined as:

$$Skewness = \frac{\sum_{i=1}^{n} \frac{(x_i - \mu)^3}{n}}{\sigma^3}$$

Where, x_i are the data points of the distribution, μ is the mean, σ is the standard deviation of the distribution. While n is the sample size.

3.1 Classification using ML algorithms

3.1.1 Linear Discriminant Analysis

Linear discriminant analysis (LDA), is a generalization of Fisher's linear discriminant, it is a method used in statistics, which finds a linear combination of those features which separates two or more classes of objects. It is a special case of QDA in which the Gaussians for each class are assumed to have the same covariance matrix, also it assumes a normal distribution of data. "The main goal of LDA is to look for a vector (V) in feature space in such a way that the two projected clusters of decision-Yes(Y) and decision-No (N) on V-direction can be well separated from one another, while small variance for both clusters is maintained. Dimensionality reduction

using LDA is achieved by three steps, First step includes the calculation of Between-class variance. The second step calculates with-class variance". The third step is the construction of a lower-dimensional space and is given as:

$$P_{lda} = \arg\max_{P} \frac{\left| P^T S_b P \right|}{\left| P^T S_w P \right|}$$

3.1.2 k-nearest neighbor (k-NN)

KNN is a non-parametric technique proposed by Thomas cover. It is widely used for different classification, matching, recognition and regression tasks. In classification case, a class label is an expected output, that label is assigned to the object depending on which is the most common class in its K-nearest neighbors. It has certain advantages of being simple, easily implementable, and robust to noisy training data, also as it is a non-parametric method so there is no need to build a model, make any assumptions or tune any parameters. Major disadvantages of using KNN classifier include its high computational cost, determination of K value, and slowness of Algorithm if it is subjected to a large number of examples.

$$D(x,p) = \begin{Bmatrix} \sqrt{(x-p)^2} & \text{Euclidean} \\ (x-p)^2 & \text{Euclidean Squared} \\ (x-p) & \text{Manhattan} \end{Bmatrix}$$

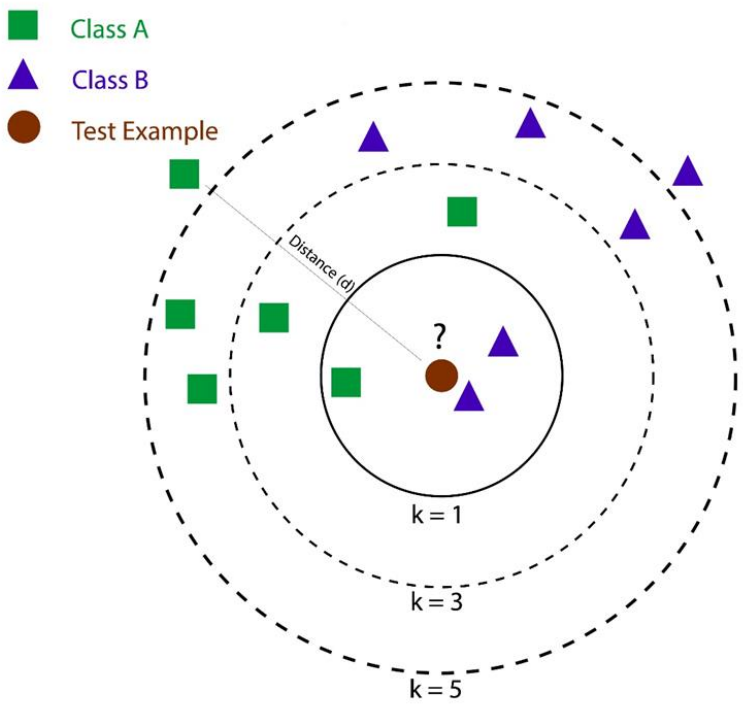

Figure 3-1: k-NN Classifier

3.1.3 Support vector machines (SVM)

SVM is also one of the supervised machine learning algorithms that are widely used for classification problems as well as for regression problems and pattern recognition tasks. With a labeled training dataset given. "The main goal of SVM is to find a hyperplane in an N-dimensional space, (where N is the no. of features) that decidedly classifies data points, many hyperplanes can be chosen to separate the two classes of data points" [89]. Thus, the main objective of SVM is to find a plane out of all possible hyperplanes that have the maximum distance with the data points from both classes. SVM works efficiently for higher-dimensional space problems and is also memory efficient. For a two-dimensional feature space, hyperplane is given by:

$$f(x) = r.x + b$$

Where b is a scaling while the cost function is given by:

$$J(\theta) = \sum_{i=1}^{m} y^{(i)} Cost_1\,(\theta^T(x^{(i)}) + (1 - y^{(i)}) Cost_0(\theta^T(x^{(i)})$$

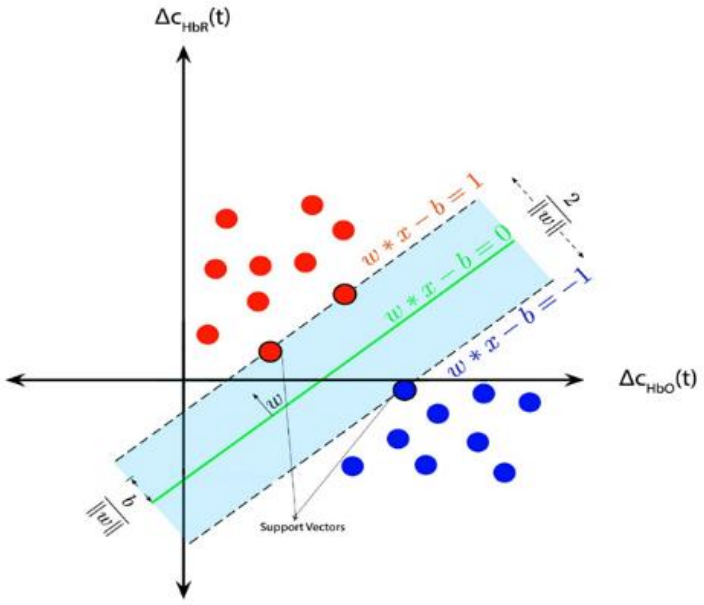

Figure 3-2: Hyperplane in 2-dimensional feature space in Support Vector Machine

3.2 Classification using DL algorithms

3.2.1 Artificial neural networks (ANN)

ANNs are artificial computing systems, commonly used in machine learning and data mining that are inspired by biological neural networks. ANNs learn to perform a specific task without being programmed with specific task rules through provided training data. Training data is like examples of the given task needed to be performed by the ANNs. Most commonly ANNs are used in image recognition, where the designed network learns to differentiate between different images of specified classes. Training data set in this case have two to three classes with hundreds of images of a specified class along with the class label. Designed ANN learns the features from the training dataset without any prior knowledge of objects of a specific class. These trained networks are then used for image recognition when provided with an unknown dataset of objects of different classes.

The output of a single neuron is given by:

$$a_i^{(j)} = g(\theta^{(j)} x_k)$$

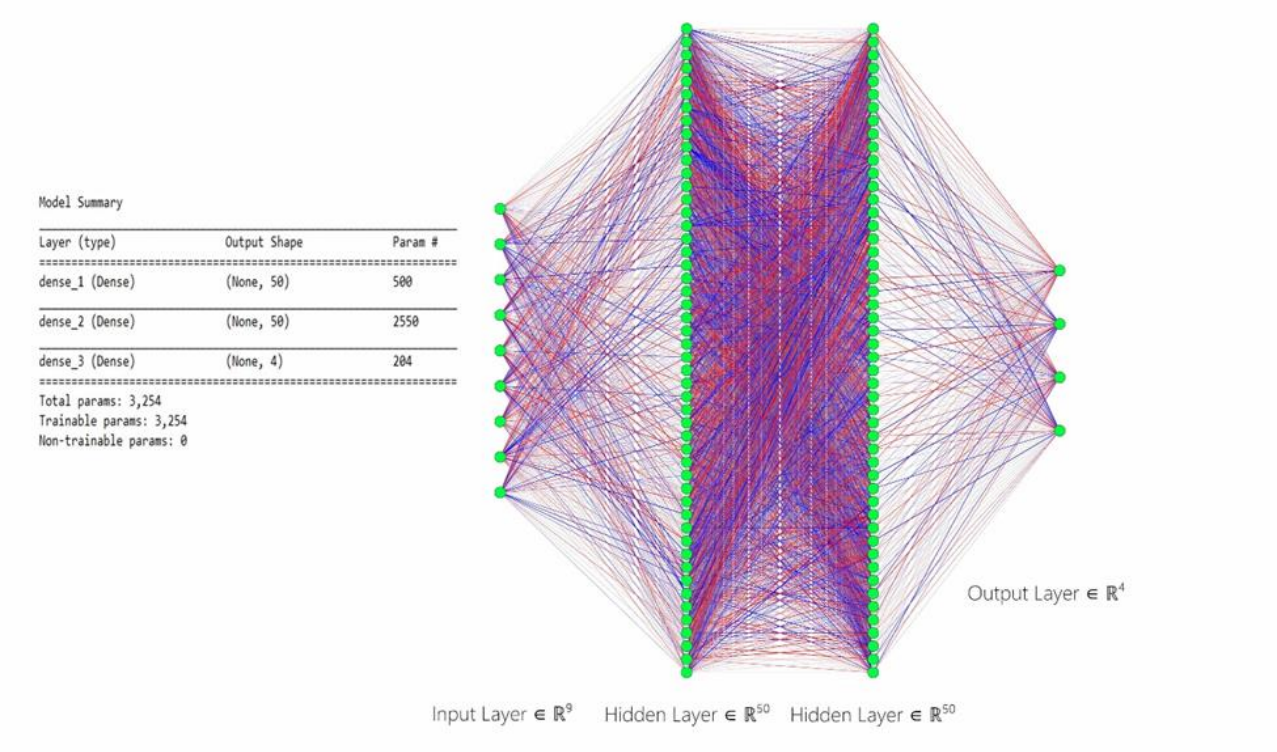

Figure 3-3: Model summary of Artificial Neural Network

3.2.2 Convolutional Neural Networks (CNN)

CNN is a multi-layered neural network with architecture to detect the complex features in the data. "Unlike the traditional multi-layer perceptron architectures, CNN uses two operations called 'convolution' and 'pooling' to reduce the image into its essential features, and then uses those features for understanding and classification of the image" [117]. CNNs are made up of some basic building blocks. These blocks include Convolutional Layer in which a filter or kernel is passed over an image, Activation Layer has normally an activation function "ReLu", this layer introduces nonlinearity that allows the network to train itself through backpropagation. Pooling layer down-samples and reduces the size of the matrix, it focuses on the most prominent information in each feature of the image. The last one is named the fully connected layer, this layer outputs the different probabilities associated with every label attached to the image. The label with the highest probability is the classification decision. CNNs are widely used in agriculture, self-driving vehicles, healthcare, and surveillance.

$$Output\ \text{size}(\text{W}, \text{H}) = \frac{(\text{N-F})}{\text{stride}} + 1$$

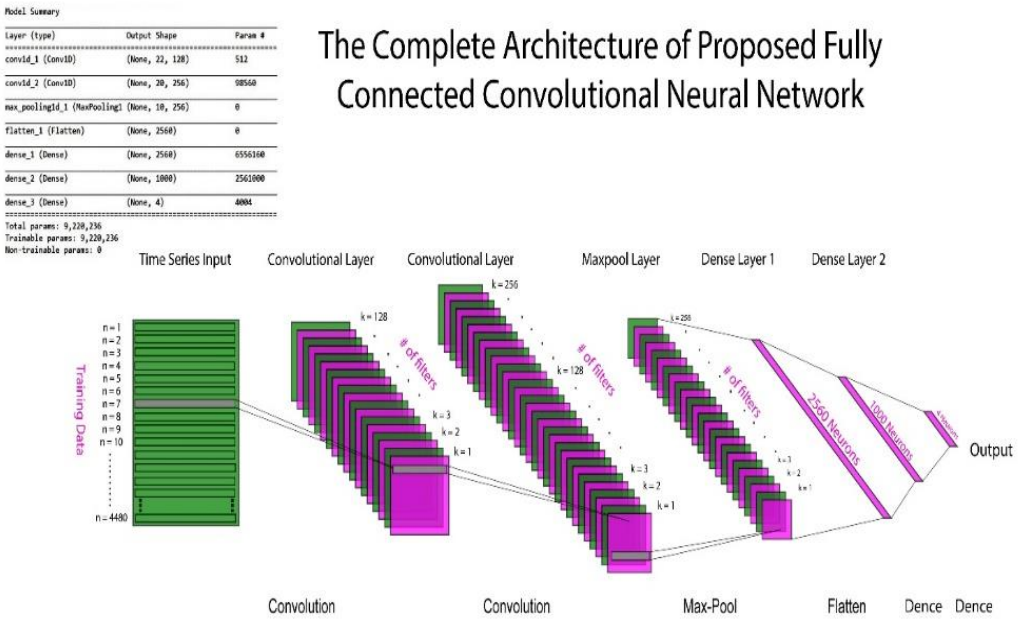

Figure 3-4: Complete architecture and Model summary of Convolutional Neural Network

3.2.3 Long Short Term Memory (LSTM)

LSTM or Long short term memory networks are the type of Recurrent Neural Networks that uses some special unit in addition to the standard units. These special units include the "memory cell" that maintains information in its memory for a longer period. LSTM has feedback connections unlike the standard feed-forward neural networks, it can process the whole sequence of data i.e. speech, video, etc. LSTM is used widely in speech recognition, handwriting recognition, handwriting generation, Music generation, Language translation, image captioning, and anomaly detection in intrusion detection systems. A simple LSTM unit is made up of a cell, input gate, output gate, and forget gate. The cell remembers the information whereas gates regulate the flow of information. LSTM networks are modified forms of RNN, they remember the past data in memory. The logistic sigmoid function for the LSTM memory cell is given by:

$$f(x) = \frac{1}{1 + e^{-k(x - x_0)}}$$

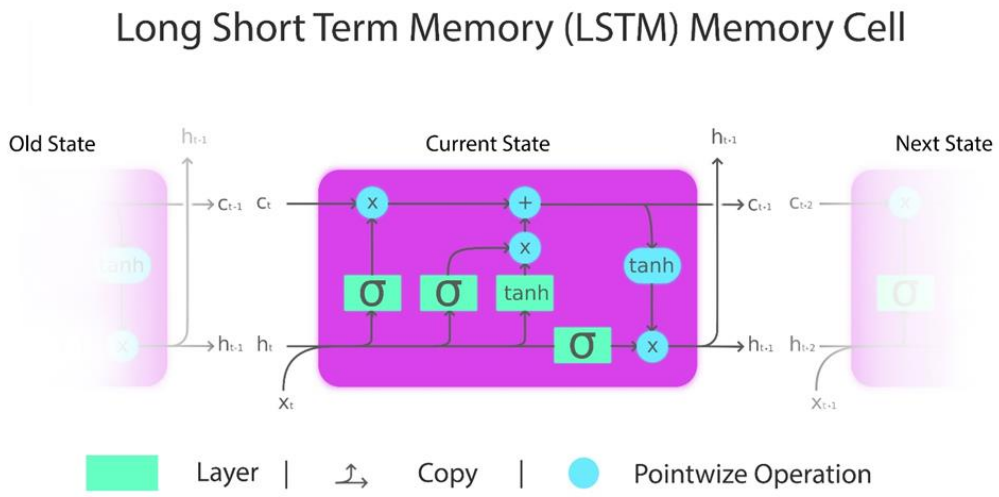

Figure 3-5: Architecture of a Memory Cell of Long Short Term Memory Network

3.4 Results

The application of deep learning (DL) algorithms is a relatively new field for fNIRS data classification and many of its dimensions are yet to be explored. DL algorithms don't require manual feature engineering. Estimation and classification of 4 levels of MWL using logic, coding, and mental arithmetic tasks for the first time in research history on MWL makes this work novel from others along with the implementation of LSTM on 4 levels of MWL -fNIRS data with optimum classification accuracy results. In CNN, convolutional layers automatically extract those features having classifiable information. CNN outperformed all ML classifiers by an acceptable margin. Neuroergonomics application of LSTM is novel in DL for MWL-fNIRS data. Table 2 summarizes the results of all participants in terms of their classification accuracies, precision, and recall.

Table 3-1: Artificial Neural Network result: accuracies, precision and recall of subjects

S1			**S2**			**S3**		
Accuracy	Precision	Recall	Accuracy	Precision	Recall	Accuracy	Precision	Recall
79.76	85.71	81.63	77.42	82.54	77.84	69.87	78.83	70.07
S4			**S5**			**S6**		
Accuracy	Precision	Recall	Accuracy	Precision	Recall	Accuracy	Precision	Recall
67.79	73.57	67.91	55.71	72.71	55.84	78.07	85.79	78.22
S7			**S8**			**S9**		
Accuracy	Precision	Recall	Accuracy	Precision	Recall	Accuracy	Precision	Recall
79.40	83.97	81.88	56.62	74.69	56.72	64.30	76.92	64.47
S10			**S11**			**S12**		
Accuracy	Precision	Recall	Accuracy	Precision	Recall	Accuracy	Precision	Recall
78.44	84.46	78.63	74.38	79.84	74.54	57.59	72.79	57.76
S13			**S14**			**S15**		
Accuracy	Precision	Recall	Accuracy	Precision	Recall	Accuracy	Precision	Recall
67.78	78.28	67.97	60.04	73.54	60.06	65.21	77.52	65.26

Classification results from the LSTM classifier are represented in Table 3. Comparing the results of table 2 and table 3, shows that the highest accuracy achieved using CNN classifier is 93.02 %, while the highest accuracy with LSTM classifier is 95.51%, which means that LSTM results in higher classification accuracy as compared to CNN.

Table 3-2: Classification accuracies, precision and recall achieved with selected CNN model

S1			**S2**			**S3**		
Accuracy	Precision	Recall	Accuracy	Precision	Recall	Accuracy	Precision	Recall
75.31	77.58	75.63	86.82	87.41	87.16	82.81	83.43	82.81
S4			**S5**			**S6**		
Accuracy	Precision	Recall	Accuracy	Precision	Recall	Accuracy	Precision	Recall
71.92	73.59	71.66	86.77	87.60	86.95	86.66	87.65	86.81
S7			**S8**			**S9**		
Accuracy	Precision	Recall	Accuracy	Precision	Recall	Accuracy	Precision	Recall
79.79	81.69	80.18	84.32	84.68	84.62	77.34	77.09	77.59
S10			**S11**			**S12**		
Accuracy	Precision	Recall	Accuracy	Precision	Recall	Accuracy	Precision	Recall
81.77	83.54	81.90	79.21	79.76	79.54	80.61	83.75	82.19
S13			**S14**			**S15**		
Accuracy	Precision	Recall	Accuracy	Precision	Recall	Accuracy	Precision	Recall
81.61	83.74	81.42	77.98	78.91	77.98	87.55	88.32	87.68

Table 4 represents a detailed comparison of results between ANN, CNN, and LSTM in box plots.

Table 3-3: Classification accuracies, precision and recall achieved with proposed LSTM network

S1			**S2**			**S3**		
Accuracy	Precision	Recall	Accuracy	Precision	Recall	Accuracy	Precision	Recall
83.69	85.34	83.84	88.80	89.53	89.12	88.43	88.68	88.51
S4			**S5**			**S6**		
Accuracy	Precision	Recall	Accuracy	Precision	Recall	Accuracy	Precision	Recall
83.80	84.03	83.86	91.71	92.16	91.84	92.34	93.38	92.44
S7			**S8**			**S9**		
Accuracy	Precision	Recall	Accuracy	Precision	Recall	Accuracy	Precision	Recall
88.17	88.25	88.37	86.25	86.65	86.40	85.26	85.66	85.49
S10			**S11**			**S12**		
Accuracy	Precision	Recall	Accuracy	Precision	Recall	Accuracy	Precision	Recall
89.16	89.76	89.28	83.43	83.68	83.72	74.32	77.88	74.63
S13			**S14**			**S15**		
Accuracy	Precision	Recall	Accuracy	Precision	Recall	Accuracy	Precision	Recall
88.59	89.79	88.68	85.10	86.81	85.06	91.04	90.95	90.12

This result of the carried research shows that LSTM is an optimum classifier for MWL classification using fNIRS brain signals resulting in high classification accuracies ranging between 74.32 -92.34%. Estimation and classification of 4 levels of MWL using logic, coding, and mental arithmetic tasks for the first time in research history on MWL makes this work novel from others along with the implementation of LSTM on 4 levels of MWL -fNIRS data with optimum classification accuracy results. Estimation and classification of 4 levels of MWL using logic, coding, and mental arithmetic tasks for the first time in research history on MWL makes this work novel from others along with the implementation of LSTM on 4 levels of MWL -fNIRS data with optimum classification accuracy results.

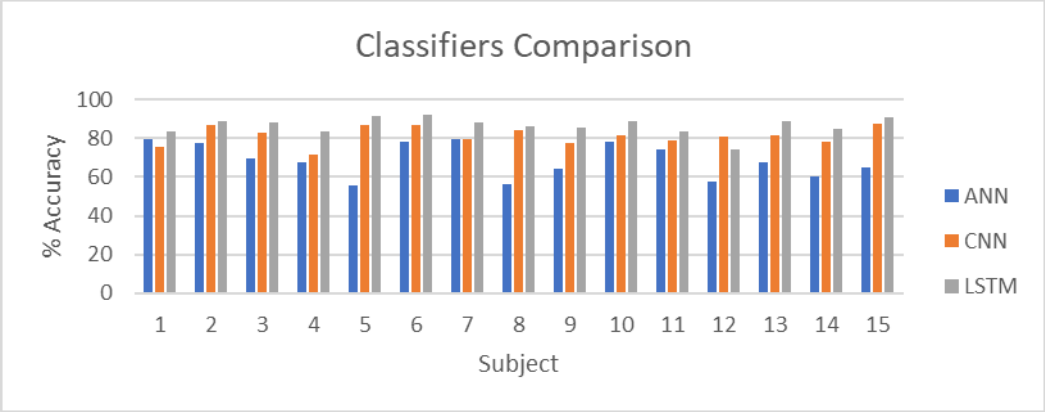

Figure 3-6: Comparison of classification accuracies of subjects between ANN, CNN, and LSTM

CHAPTER 4: COMPARISON BETWEEN MACHINE LEARNING AND DEEP LEARNING COMPUTATIONAL RESOURCES

In Human-Machine Interaction (HMI), Neurorobotics, Neuroscience, Rehabilitation and Assistive Robotics (RAR) different noninvasive measures like EEG, fMRI, PET, and fNIRS are being used to measure the brain activities in certain regions for further employment in Brain-Computer Interface (BCI) and neuroergonomics[43], [65], [76][77][78]. In HMI and neuro-ergonomics primary focus is on the relationship between the nervous system and its impact on human emotions, decision making, physiology, cognition, behavior, and optimizing interaction with intelligent machines in real-time scenarios [1][4]. RAR mainly deals with the use of brain signals to generate control commands and use them to operate external devices [65][18]. RAR enables paralyzed locked-in patients, or people suffering severe motor disabilities to communicate and control external controls such as robotic arms and prostheses [79][80]. Nowadays, the use of BCI has seen in everyday activities from controlling external devices, monitoring cognitive states, estimating passive brain activities (e.g. drowsiness detection), games theory, neuromarketing, smart environment, education, self-regulation, and security [81][82][83][84]. The efficient use of BCI is subjected to robust signal acquisition from the brain and correctly classifying these obtained signals [85]. Methods used to acquire brain signals can be invasive, semi-invasive, or non-invasive [4]. In an invasive method, micro-electrodes are placed straight into the cortex through the process of neurosurgery. These microelectrodes quantify the action of a single neuron. Local Field Potentials (LFPs) and intracellular potentials over extracellular action potentials (APs) are an example of invasive devices. In semi-invasive methods, electrodes are placed inside the scalp on the visible exterior of the brain. Electrocorticography (ECoG) is a commonly used semi-invasive device. In the non-invasive technique, sensors are sited on the scalp to measure the electrical or hemodynamic activity of neurons. There are several non-invasive techniques to study brain activities including EEG, fNIRS, fMRI, MEG, and PET. Non-invasive devices are most commonly used due to the fact they don't need any surgery and data could be easily acquired over a long duration of time. Within the non-invasive paradigm, there are certain inherent characteristics and properties attached to each acquisition system. PET has high temporal and spatial resolution but requires an injection of radioactive material. fMRI and MEG are huge and bulky machines and they are

fixed in a room nature limits their capabilities. fNIRS and EEG however, are lightweight easy to use, portable, and have the liberty of limited action especially in the case of fNIRS [17], [43]. Although, fNIRS and EEG struggle in temporal and spatial resolution as compared with other modalities being portable and wearable, and user friendly make them prevalent choice over other devices [86].

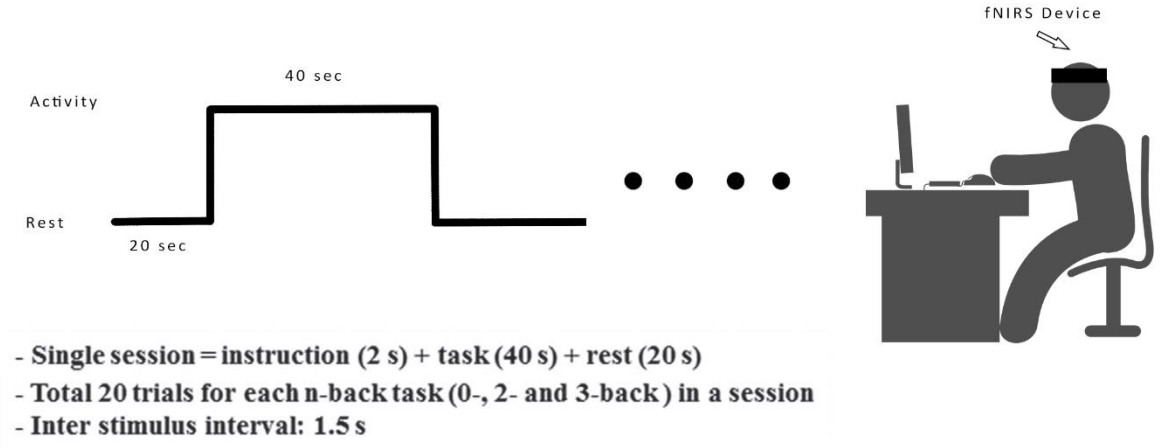

Figure 4-1: Experiment protocol for n-back task

In the current era of human-machine collaborative working environments where Human-Machine Interaction (HMI) is increasing each day and AI industrial environment has amplified the need for human factors considered while designing these collaborative setups. Among these important human factor considerations, neuroergonomics including analyses of human mental workload (MWL), stress level, and other cognitive states are vital to consider for operators' wellbeing and safety. Similarly, brain signals are becoming paramount for rehabilitation and assistive purposes in fields such as brain-computer interface (BCI), closed-loop neuromodulation for neurological disorders, etc. The fNIRS has immerged as a potential non-invasive neuroimaging solution to monitor brain states for said purposes. An essential part of the design of such a mental state assessment system is to correctly classify the acquired brain signals in a reasonable time.

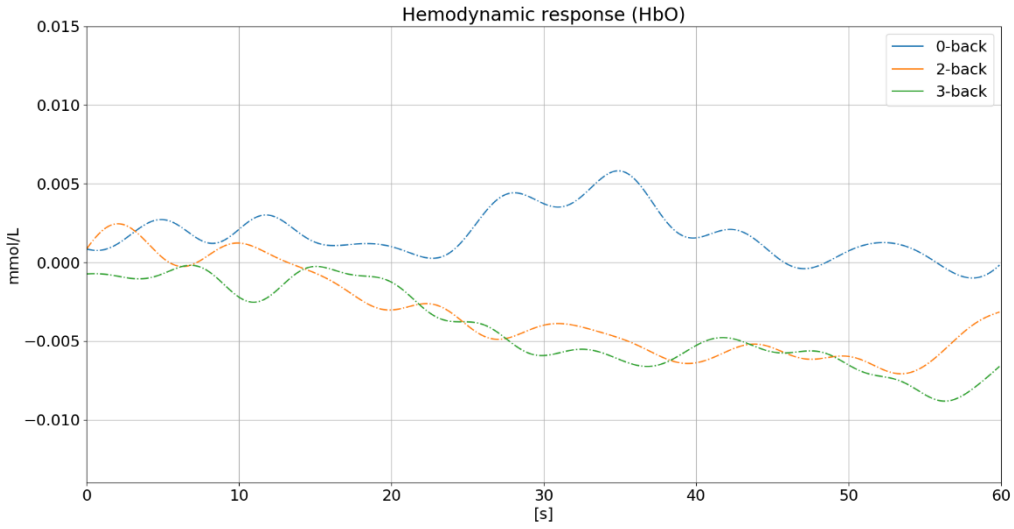

Figure 4-2: Hemodynamic response (HBO) for n-back tasks

Deep Learning (DL) for such classification purposes due to feature engineering and complex data pre-processing requirements of machine learning algorithms. Bypassing the challenges of feature engineering through DL techniques comes at the cost of time and computational complexity of the system. We utilize the fNIRS recordings and perform MWL classification using conventional LDA, k-NN, SVM, and DL algorithms ANN, CNN, and a recurrent neural network LSTM. In this study, we discussed the theoretical computational complexities and compared generalizability, classification accuracies, train and test time requirements of k-NN, SVM, ANN, CNN, and LSTM. The averaged accuracy achieved using k-NN, SVM, ANN, CNN, and LSTM is 92.54 , 81.47, 64.80, 55.94, 58.61, and 32.13 % while averaged train time being 127.40, 7.57, 1.41, 0.45, 0.01, and 0.03 sec and test time being 0.603, 0.040, 0.038, 0.039, 0.061, and 0.00032 sec, respectively. The findings suggest that ML algorithms are recommended for real-time BCI with low commands and focus on efficient computation while DL algorithms are recommended for use cases where high commands and accuracy are of prime importance. CNN covers the nice ground between optimal classification accuracy and reasonable train, test time.

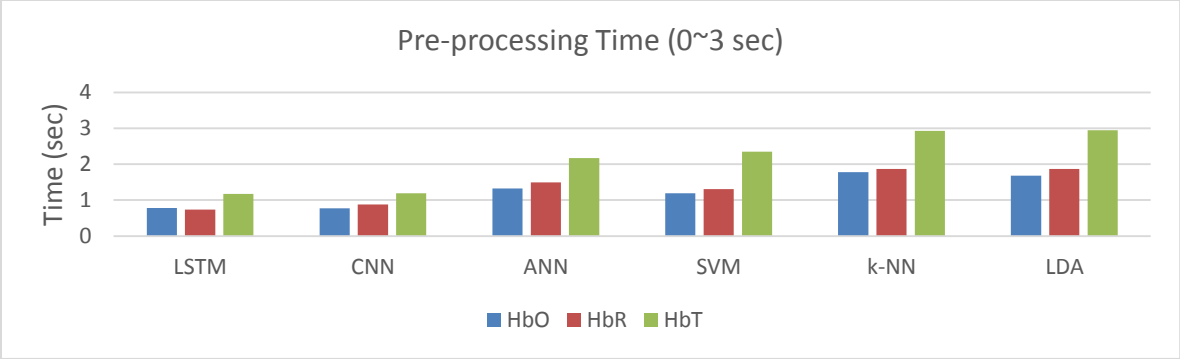

Figure 4-3: Pre-processing time of HbO, HbR, and HbT for 0-3 sec window of LSTM, CNN, ANN, SVM, k-NN, and LDA

4.1 Computation Complexity

In this section, we will present theoretical grounding and benchmarks for all conventional, ML, DL, and RNN algorithms. The computational complexity of the model usually includes Time complexity and Space complexity and is often expressed using the Big O notation. The Big O notation defines an upper bound of an algorithm and is used to classify algorithms according to their run time or space requirement that increases as the input tensors grow [87].

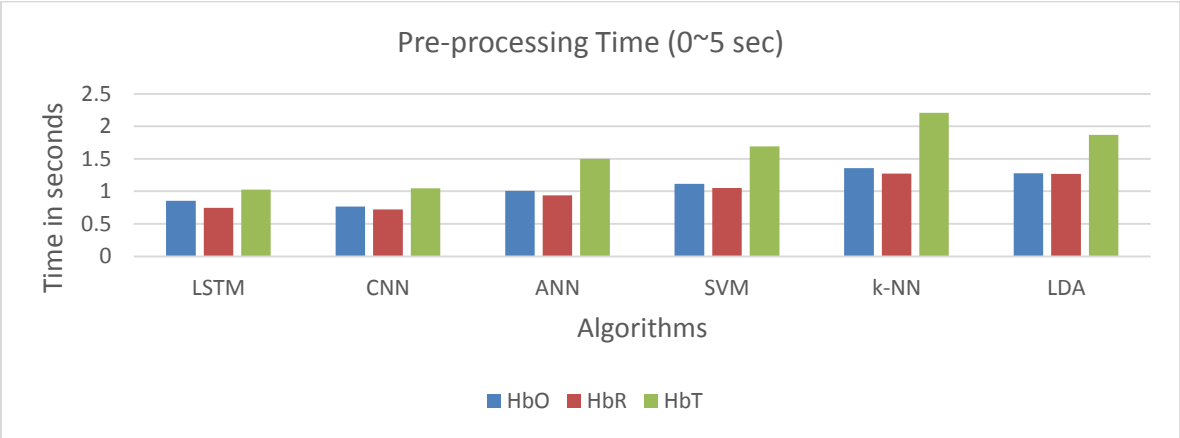

Figure 4-4: Pre-processing time of HbO, HbR, and HbT for 0-5 sec window of LSTM, CNN, ANN, SVM, k-NN, and LDA

Let *N* be the number of training examples, *M* is the features of the data, *R* is the number of iterations, *d* is the number of dimensions of the data and *k* is the number of neighbors (in case of k-NN). The computation complexity of k-NN is *O(kNd)* [35]. The time is linear for the

number of instances and dimensions. The k-NN algorithm is a non-parametric machine learning algorithm, hence it doesn't make strong assumptions about the form of the mapping function and learn the functional form from the training instances for later comparison with test instances. It is the only algorithms among the considered algorithms hence it required space complexity as well for the complete description and is O(Nd) [36]. In the case of LDA, there are two different possibilities for computational complexities that depends on the fact that if the number of features is greater than the training example or not. In the former case, the computational complexity of LDA is $O(Nd^2)$ while in the latter case it is $O(d^3)$ [35][88]. The computational complexity of non-linear and non-approximate SVM is $O(N^2)$ or $O(N^3)$ depending on the type of selected kernel while the computational complexity of approximate SVM is $O(NR)$ [35].

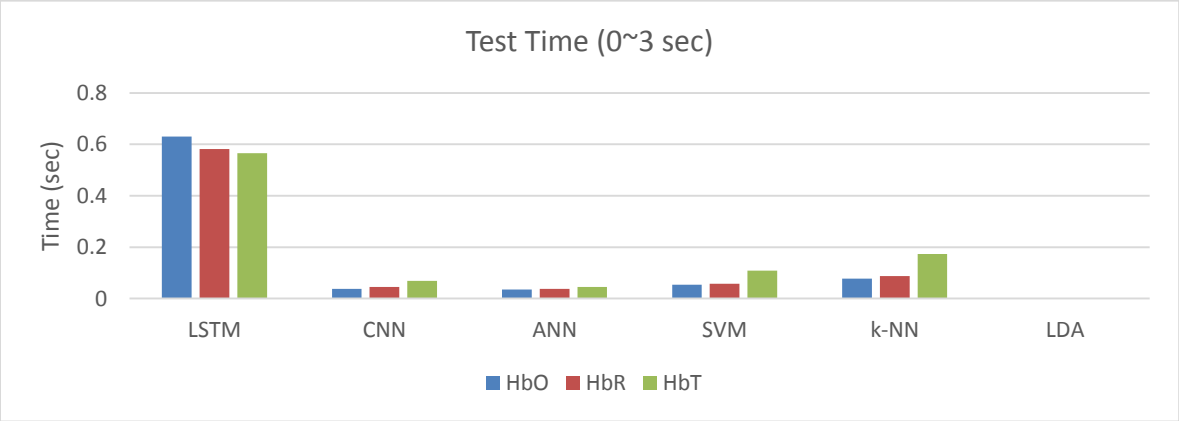

Figure 4-5: Test time of HbO, HbR and HbT for 0-3 sec window of LSTM, CNN, ANN, SVM, k-NN and LDA

The computation complexity of deep neural networks (ANN, CNN, and LSTM) is highly architecture-dependent, similar to "Output sensitive" algorithms [89]. For ANN, "let's i denotes the number of nodes of the input layer, j the number of nodes in the second layer, k the number of nodes in the third layer, and l the number of nodes in the output layer, with t training examples and n epochs, computational complexity is given by $O(nt*(ij+jk+kl))$" [88]. For CNN, "Let's assume a group of g kernels of size $u \times v$ is applied to f feature maps of dimension $m \times n$, p_m and p_n are the amounts of zero-padding on the borders of input feature maps, while filters are applied with a stride of s". The dimensions of the output feature map in the m and n directions can be written as $o_m = (m - u + 2p_m) / s + 1$ and $o_n = (n - v + 2p_n) / s + 1$, the computational complexity is given by $O((f \times u \times v+1) \times g \times o_m \times o_n)$ [90].

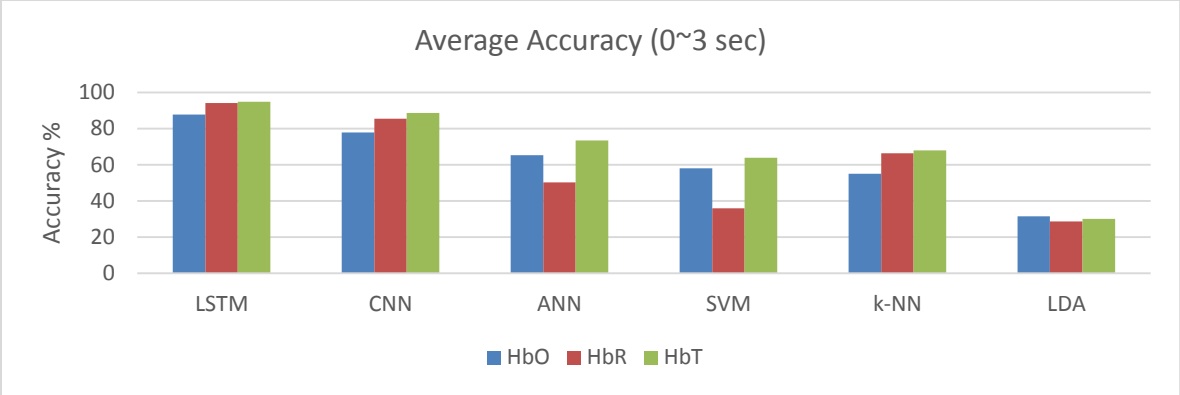

Figure 4-6: Average Accuracy of HbO, HbR and HbT for 0-3 sec window of LSTM, CNN, ANN, SVM, k-NN and LDA

There are different proposed complexity measure for RNN [91][92]. Generally, the architecture complexity of RNNs might be measured by recurrent depth or the feedforward depth, please read [92]. These theoretical computational complexities (both time and space), however, does not reflect the complete picture. Usually, the DL algorithms perform matrix multiplication and are massively parallelize and scaled across a huge number of distributed systems for training, testing, and inference. Therefore, the applied DL stats differ from theoretical results depending upon the used hardware (CPU, GPU, TPU, ASIC, FPGAs, etc.), optimizing compiler for manipulating and evaluating mathematical expressions (Tensorflow, Theano, Chainer, THNN, MaxNET), parallel computing platforms (CUDA, Vulkan, OpenGL, OpenCL) and other software and hardware nuances. This study is primarily designed to take into account all these ground truths and recommend the appropriate learning algorithms for a given problem at hand.

4.2 Results

The results of different classifiers along with their obtained accuracies and computation time for HbO, HbR, and HbT signals are presented in this section. A total of 26 participants took part in this study. The data acquisition and initial cleansing includes conversion of acquired light densities into hemodynamic response using Modified-Beer Lambert law and applying for zero-phase low pass, 6th order Butterworth filter. These steps are mandatory and are the same for all of the listed algorithms, that's why they are not included in computation time. As discussed earlier, the analysis is performed for HbO, HbR, and HbT signals. Three different time windows

of lengths 0~3 sec, 0~5 sec, and 0~10 sec with 20% overlap were used to segment the pre-processed signals. For machine learning classifiers and ANN, after segmentation, the feature engineering phase begins. There are a lot of possible features that can be extracted in the temporal, spectral, and wavelet domain. Due to the dynamic nature of the brain signals, different experimental paradigms, and varying signal source locations, we have to compute the best performing features every time. That's why complex feature engineering is considered as the bottleneck for ML classifiers. Numerous studies have explored the feature engineering domain for machine learning classification. For our analysis, we have chosen signal mean and signal peak as features for machine learning algorithms [ ], while CNN and LSTM self-extract the features. For sake of completeness, we used both HbR and HbT alongside HbO in data analysis, but HbO will be the major focus of discussion and comparison due to its de facto used. Last but not least, it turns out that there is a huge discrepancy between key evaluating parameters spanning up to 8 decimal digits after zero. We used a clever workaround to overcome this nuance and present comparison results in a much readable and easy to understand format. First, we present respective accuracy on the test set and computational times w.r.t to the train and test (having split ratio i.e. 70:30) instead of per sample results. Second, in each comparison category, the highest and lowest values are scaled by dividing each value by the lowest in that category [23].

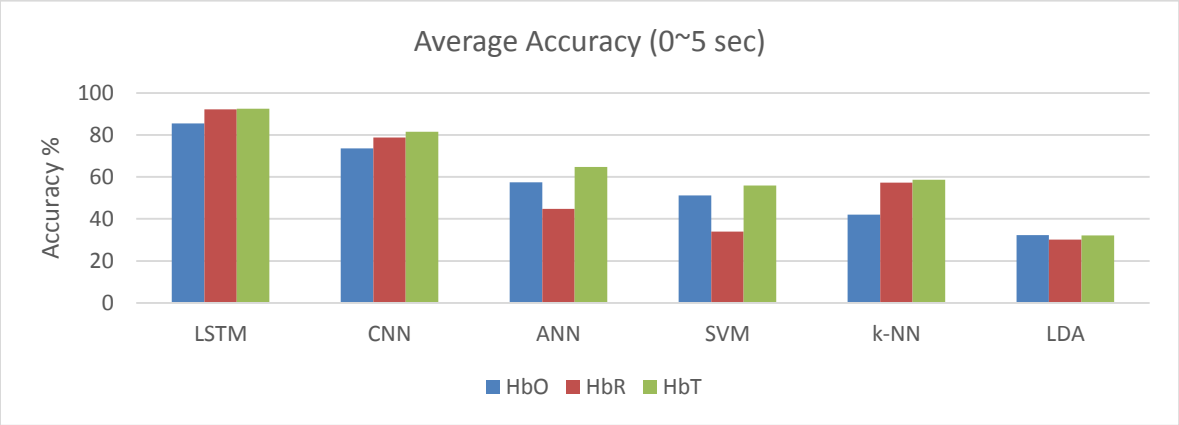

Figure 4-7: Test time of HbO, HbR and HbT for 0-5 sec window of LSTM, CNN, ANN, SVM, k-NN and LDA

Among the classification classifiers, the pre-processing phase is different depending upon the fact if manual feature extraction is performed or not [86], [93]. For all ML classifiers and ANN, manual feature engineering is required, this elevates their pre-processing time by almost 2

times more than CNN and LSTM that do not require feature engineering. Pre-processing time has an inverse relation with window size, the smaller the window size the more samples will be there to calculate features from and vice versa. Figure 4(a) & (b) depict this phenomenon. The results prove that indeed feature engineering is a bottleneck for ML classifiers both in terms of domain knowledge, and computing time. The self feature extracting DL algorithms have a clear margin over other classifiers.

4.3 Discussion

The training time for all algorithms is presented in Figure 5(a) & (b) for both 0~3 and 0~5 sec windows, respectively. Among all of the algorithms, k-NN is the fastest because it doesn't perform any complex calculation and just stacks the training samples together according to the similarity measure. Next in line is LDA that takes just 4 times more time to train than k-NN. While the DL algorithms take subsequently very long time to train. SVM, ANN, and CNN take almost 90, 320, and 730 times, more time to train as compared to k-NN, respectively. LSTM implements backpropagation through time over multiple time instances recursively, with far more parameters to tune than any other algorithm. This is clearly reflected in training time as LSTM takes almost 18,000 times longer to train than k-NN. This difference is even more extreme in a 0~5 sec window where it takes more than 33,000 times more to train due to the tuning of the additional number of features through backpropagation in each sample. While remaining algorithms perform slightly better in 0~5 sec window as compared to 0~3 sec window. In this study, we implemented the conventionally used machine learning (LDA, k-NN, and SVM) and deep learning (ANN, CNN, and LSTM) algorithms on fNIRS based study on 26 subjects performing mental workload activity.

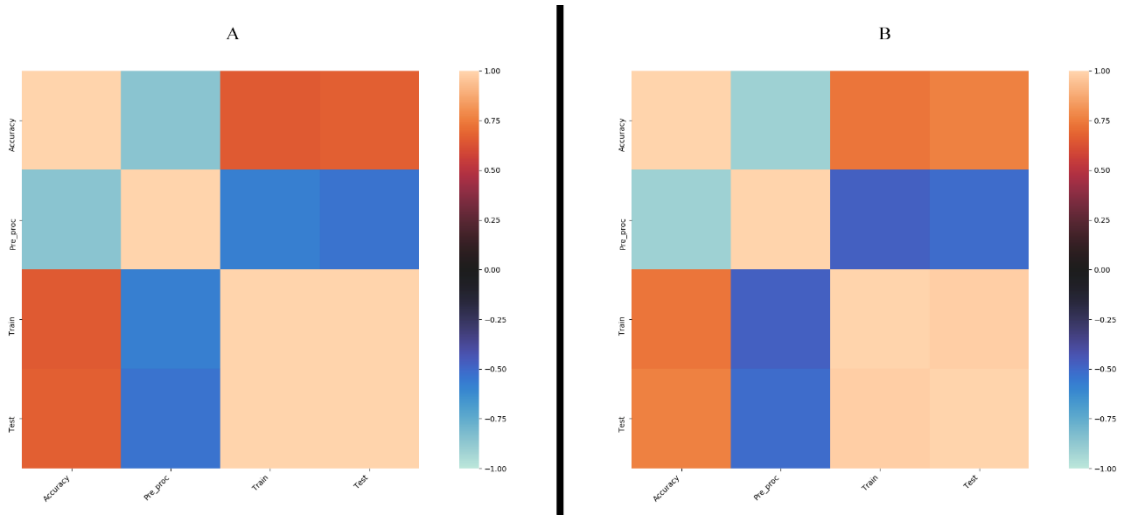

Figure 4-8: Training time for all algorithms for (a) 0~3 & (b) 0~5 sec windows

We discussed the theoretical computation complexity of all of these algorithms in terms of big O notation and then compared the practical processing time, train time, and test time complexity and requirements. The finding suggests that in terms of time requirements, the machine learning algorithms are the fastest. Within machine learning algorithms, LDA is the least compute-intensive algorithm while SVM and k-NN depend on the applied kernel and numbers of training samples, respectively. However, as proved in literature, the downside of machine learning algorithms is that their accuracy and generalizability decrease with an increase in the classification commands, in addition to the fact that they mostly rely on handcrafted feature extraction and require domain knowledge. Among deep learning algorithms, the time complexity of ANN and CNN is comparable but in terms of the accuracy department, ANN entirely depends upon the handcrafted features while CNN has impressive self-feature extraction going on. The recurrent neural network is very new in the field and few studies are performed yet, but they have shown amazing accuracies as compared to the rest of the algorithms. But the catch is that they are so compute-intensive in terms of train and test time that they might not be feasible yet for the real-time BCI. The RNN variant, LSTM is tested in this study and we conclude that they are by far the best choice for the offline brain signal analysis. The CNN covers the sweet spot as of now and offers a compromise between the accuracy and time requirement. While machine learning algorithms are still recommended for real-time applications primarily designed to work without any delay.

CHAPTER 5: SYMMETRIC HOMOGENOUS FEATURE BASED TRANSFER LEARNING FOR BCI

Brain-Computer Interface (BCI) provides a means of communication between the brain and external devices by recognizing the brain activities using brain generated signals and translating them into external commands. Recently, the use of functional near infra-red spectroscopy (fNIRS) has increased as the common non-invasive modality for brain activity detection. With higher BCI protocols more commands can be generated with good accuracy in less time. The recent trends show that deep learning has enhanced the performance of the BCI systems significantly in the following years [117]. But the inherent bottleneck for deep learning in the domain of BCI is the requirement of the huge amount of training data and computational resources for training deep networks. The collection of data is complex and expensive that makes it extremely difficult to build a large-scale, high-quality annotated dataset for training. Transfer learning might resolve the problem of insufficient training data in BCI. Transfer learning tries to transfer the knowledge from the source domain to the target domain by learning the different underlying shared patterns. In this study, we have applied symmetric homogenous instance-based transfer learning to the convolutional neural network on fNIRS-based n-back data collected from 26 participants. We explored the potential application of the transfer learning approach for the classification domain to reduce the training time and calibration time for the fNIRS-based BCI systems. The results confirmed that applying the proposed feature-based transfer learning algorithms leads to achieving the maximum accuracy of 20 epochs sooner than the conventional methods. The proposed transfer learning method also outperformed the averaged accuracy achieved using the learned CNN model over the traditional CNN model by 12% (report max accuracy).

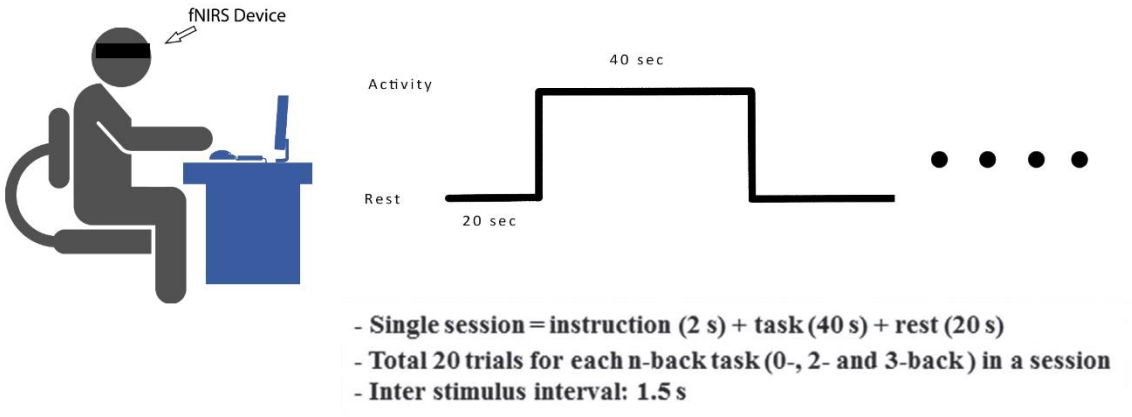

Figure 7-1: Experiment protocol for n-back task

BCI provides a method of communication between the brain and external devices through signals generated from the brain without the involvement of the peripheral nervous system [18]. BCI is among such neurofeedback methods that can improve them of patients suffering from severe motor disabilities due to tetraplegia, stroke, ad other spinal cord injuries [19]. BCI has also applications in neuro-rehabilitation, communication and control, motor therapy and recovery, brain monitoring, and neuro-ergonomics [4][20][21]. The major non-invasive BCI modalities include MMEG, FIRS, EEG, PET, SPECT and etc. Among these non-invasive BCI modalities, EEG and fNIRS are good for expense and handiness [17][22]. EEG measures brain activity by calculating the voltage fluctuations from neurons' action potentials while fNIRS detects the brain activity with reference to the changes in hemodynamic response [23][24].

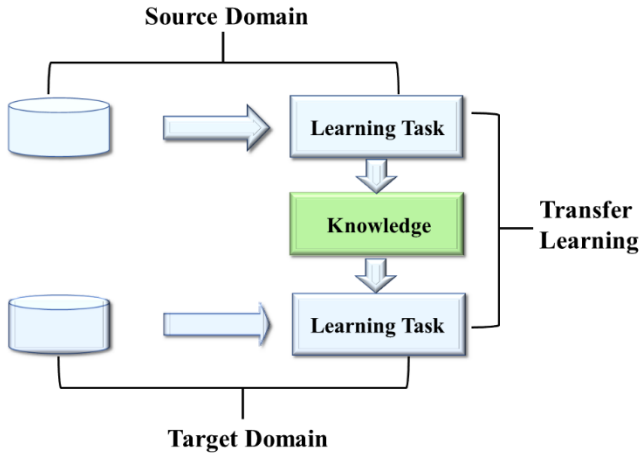

Figure 5-2: Transfer learning from source to the target domain

To use BCI out of the laboratory on daily basis, BCI needs to address several challenges such as robust signal acquisition, extracting valuable information from unrefined brain signals for control-commands, etc [25][26]. Another main problem is the necessity of recalibrating the BCI system for every single new session and the subject. Typically, the calibration time for EEG and fNIRS based BCI systems might take up to 20 or 30 minutes for all new sessions [27][28]. The obtained results after experimentation and statistical analysis are presented in this section. For framework 1, the trained CNN is used for training on the control group. Figure 1 shows the accuracies of control group subjects with training epochs. Fig 3 shows the accuracies of baseline group subjects that are trained on the randomly initialized CNN network. Tables 1 and 2 represent the accuracies of the control group and the baseline group, respectively. The network is trained up to 60 epochs before it starts overfitting. The exact brain state depends on factors such as the mental state, concentration level, psychological states, drowsiness and fatigue, anatomical differences between subjects, and statistical variations in the data [32][33]. The instrumental noise and experimental error such as changes in the electrical resistance of the probes may be because sweating may also temper the acquired brain signals [34]. All these facts combine results in the trained classifier performing poorly on new session data. The different studies tried to address these challenges by exploiting different methods and algorithms while keeping accuracy in a reasonable range [28][35][36][37]. Transfer learning might be a promising approach to deal with this problem.

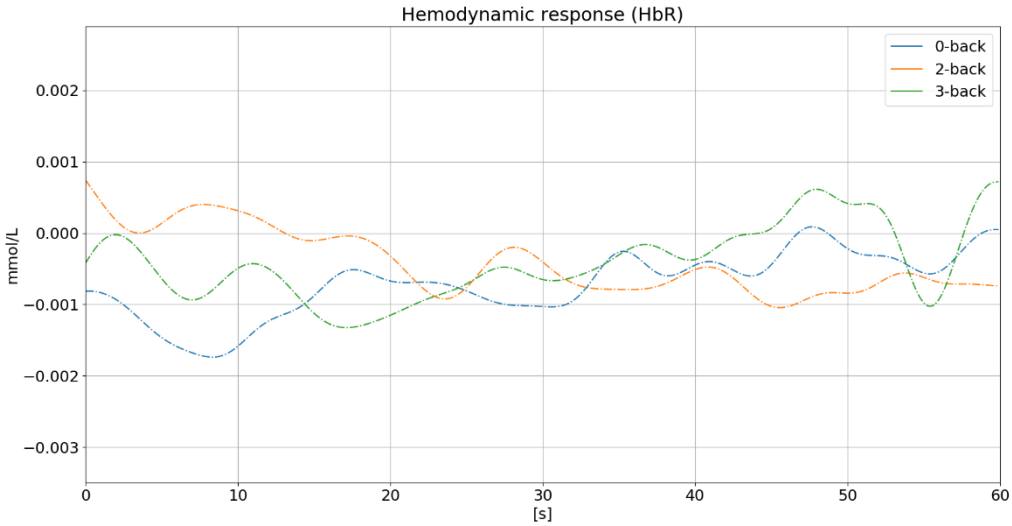

Figure 5-3: Hemodynamic response (HbR) for n-back tasks

5.1 Experiments

The available dataset of 26 participants is divided into three subsets with an approximately 60:20:20 ratio. The first 16 participants' data is used for training the CNN network that is supposed to learn the domain knowledge of the task. This trained network is then used as parameters with D_t. We evaluate the validity and viability of transfer learning under two different frameworks: 1) the transfer learning efficiently transferred the source domain knowledge to the target domain and required the reduced training iterations for deep learning models, 2) the transfer learning minimizes the need for a large amount of data required for training deep learning model for the target domain. We evaluate these two hypotheses by dividing the remaining 10 subject data into two groups having 5 participants each and named them as the baseline and control group. The baseline group is used for training conventional deep neural network models in a standard and widely adapted setting while the control group is trained on the pre-trained CNN model that is supposed to have domain knowledge from the first 16 participants. For hypothesis 1, the pre-trained model is fed with the control group data and trained with different epochs from 10 up to 60. The same steps are repeated for the randomly initialized weights CNN on the baseline group data. These obtained accuracies are compared with the baseline group accuracies and conclusions are drawn. For hypothesis 2, the data from the control group participants are fed into the pre-trained model in chunks from 10% up to 70% and accuracies are monitored if they match with are improving are not. The available dataset of

26 participants is divided into three subsets with an approximately 60:20:20 ratio. The first 16 participants' data is used for training the CNN network that is supposed to learn the domain knowledge of the task. This trained network is then used as parameters with Dt. We evaluate the validity and viability of transfer learning with two hypotheses: 1) the transfer learning minimizes the need for a large amount of data required for training deep learning model, 2) the transfer learning efficiently transferred the source domain knowledge to the target domain and required the extended training time for deep learning models. We evaluate these two hypotheses by dividing the remaining 10 subject data into two groups having 5 participants each and named as baseline and control group. The baseline group is used for training conventional deep neural network models in a standard and widely used setting while the control group is trained on the pre-trained CNN model that is supposed to have domain knowledge from the first 16 participants. For hypothesis 1, the data from the control group participants are fed into the pre-trained model in chunks from 10% up to 70% and accuracies are obtained. These obtained accuracies are compared with the baseline group accuracies and conclusions are drawn. Similarly, for hypothesis 2, the pre-trained model is fed with the control group data and trained with different epochs from 10 up to 100. The same steps are repeated for the randomly initialized weights CNN on the baseline group data.

5.2 Transfer Learning

This paper assumes that there are multiple simultaneous EEG and fNIRS acquired from different subjects, on the same and/or different tasks are available. There are many terminology inconsistencies throughout the literature regarding Transfer Learning, domain adaptation, and characterizing the transfer learning process concerning the availability of labeled and unlabeled data. "We will use the following definition throughout the paper: A domain D consists of two essential parts, a feature space also known as latent space $\boldsymbol{X}$ and a marginal probability distribution (MPD) $P(X)$, where feature vectors $X = \{x1 , \ldots , xn\} \in \boldsymbol{X}$". In the case of BCI, "the generation of command is the classification goal and the channel readings are considered as features, then x_i is the i^{th} feature vector (instance) corresponding to the i^{th} generated command, n is the number of feature vectors in X, and the $\boldsymbol{X}$ is the space of all possible feature vectors, for a given domain D, a task T can be defined as a label space Y, and a predictive function $F<.>$". The predictive function $F<.>$ is learned from the feature instance and corresponding label pairs $[x_i,$

$y_i]$ where $x_i \in X$ and $y_i \in Y$. In the case of the BCI problem, "Y is the set of labels that might be *rest, open, close* commands, y_i takes on one of the command value, and $f(x)$ is the function approximator that predicts the label value for the command classification x". From the above definitions, a data domain is given by $D = [\boldsymbol{X}, P(X)]$, and a task is given by $T = [Y, F <.>]$. Also, for consistency, we will represent source domain data as D_S and by definition, it will be given by $D_S = [(x_{S1}, y_{S1}). . . , (x_{Sn}, y_{Sn})]$, where $x_{Si} \in \boldsymbol{X}_S$ and it is the i^{th} data point of D_S and $y_{Si} \in Y_S$ is the corresponding feature label for x_{Si}. Likewise, the target domain data can be given as D_T where $D_T = [(x_{T1}, y_{T1}). . . , (x_{Tn}, y_{Tn})]$ where $x_{Ti} \in \boldsymbol{X}_T$ and it is the i^{th} data point of D_T and $y_{Ti}, \in Y_T$ is the corresponding class label for x_{Ti}. Now, the source task, the target task, the source predictive function, and the target predictive function can be represented by T_S, T_T, $F_S<.>$, and $F_T<.>$, respectively.

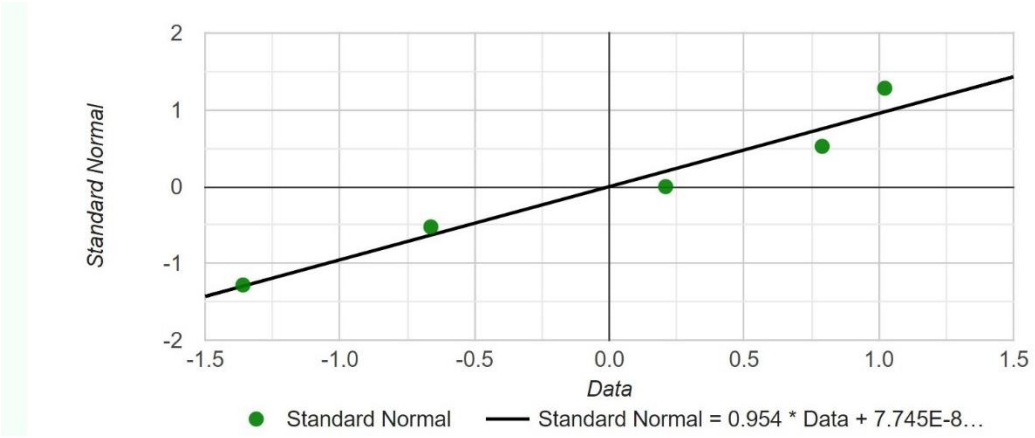

Figure 5-4: Quantile-Quantile Plot

The obtained results after experimentation and statistical analysis are presented in this section. For framework 1, the trained CNN is used for training on the control group. Figure 1 shows the accuracies of control group subjects with training epochs. Fig 3 shows the accuracies of baseline group subjects that are trained on the randomly initialized CNN network. Tables 1 and 2 represent the accuracies of the control group and the baseline group, respectively. The network is trained up to 60 epochs before it starts overfitting. Whereas the condition where the source and target domain features $\boldsymbol{X_t}$ and $\boldsymbol{X_s}$ are not equal is called heterogeneous transfer learning as shown in Fig. 1. Homogenous and heterogeneous transfer learning might be called intra-domain and inter-domain transfer learning, respectively. In this study, we will perform homogenous transfer learning on fNIRS data and evaluate its performance and viability for deep learning networks.

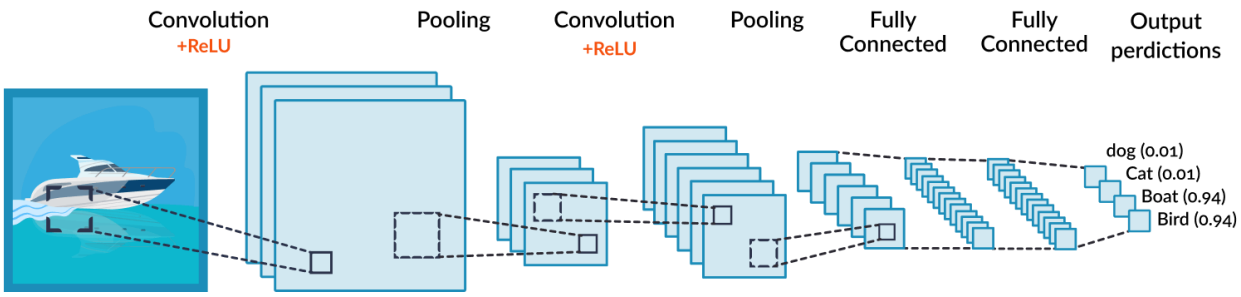

Figure 5-5: Feature learning and classification in Convolutional Neural Network

The statistical analysis is performed between baseline and control groups for both hypotheses by first confirming that the accuracies results of baseline and control group are normally distributed by the Shapiro-Wilk test. Based on the Shapiro Wilk test results, it is concluded that the statistical significance using tests such as the t-test.

5.3 Statistical Analysis

The statistical analysis is performed between baseline and control groups for framework 1 by first confirming that the accuracies results of baseline and control group are normally distributed by the Shapiro-Wilk test. The applied Shapiro-Wilk (SW) test is the test with the H0 hypothesis as data is normally distributed and H1 as data is not normally distributed. For all epoch results p-value > α, so, we here has accepted the H0. In other words, the SW test confirms that the difference between the data sample and the normal distribution is not big enough to be statistically significant. The quantile-quantile or QQ-plot is used for a graphical illustration of the Shapiro-Wilk test, Fig. 4 shows the test run on the baseline group. So SW test result tells, it is concluded that the statistical significance using tests such as t-test, and ANOVA test could be used. We used the statistical analysis to compare the classification accuracy between baseline and control groups with different hypotheses. For framework 1 the baseline and control group accuracies and the p-value is greater than 0.05 and the alternative hypothesis (H1): the two populations are not equal, a significant difference between these accuracies and the p-value is less than 0.05. After analysis, the p-value comes out to be 0.000185 and the t-value to be 3.99496 with a confidence level (α) of 95%. The result is significant with $p < 0.05$ so null hypothesis H0 is rejected.

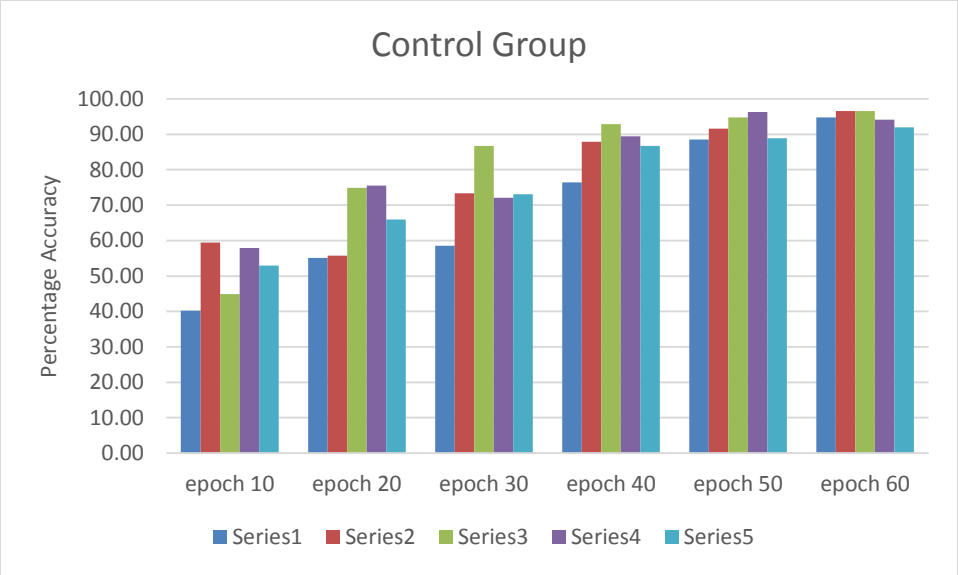

Figure 5-6: Percentage accuracy for control group for all series

5.4 Proposed Convolutional Neural Network Model

In this study, a convolutional neural network (CNN) was used to classify three mental workload classes owing to their popularity and increase in use for different studies. CNN is a deep neural network that may integrate one or more convolutional layers with a pooling layer, batch norm layer, activation layer, dense layer, and at very last an output layer. The most important layer of CNN i.e., the convolutional layer allows its inputs to pass through cascaded filters bank and performs simple convolution operations. Essentially convolution layers output feature maps extracted from the input as a result of convolution i.e., shifting and multiplication of input signal and filter. These feature maps are then used as an input to the next layer in the CNN architecture or as a set of definitive key features on which classification is performed in the last fully connected layers. The mathematical formulation of CNN layers is well explained by []. During the training of a CNN model, both filter bank parameters and dense layer weights are adjusted throughout the period so that the model precisely fits the training dataset with the least possible error. Successful implementation of CNN for a given dataset mainly relies on the fact that different data domains usually have some common key features that are shared across all of its elements (such as images). But this is not the case when it comes to generalization in areas with high inter-subject unpredictability like brain signals (EEG, fNIRS, fMRI, etc.) that differ from subject to subject and depend on a lot of external and internal factors. CNN models used for the

research were based on a feedforward CNN architecture comprising pairs of convolution and pooling layers. So, after initial tests on different feedforward CNN architectures, the chosen CNN architecture with complete parameters and structure is shown in the figure.

Table 5-1: Summary of different classifiers used in literature for different modalities

Reference	**Main category**	**Subcategory**	**Classifier**	**Modality**
[26]	Homogenous TL	Instance-based transfer learning	Bagged importance-weighted LDA	EEG
[28]	Homogenous TL	Instance-based transfer learning	Marginalized stacked denoising autoencoder	EEG
[32]		Instance-based	Selective instance transfer with active learning	EEG
[33]	Heterogenous TL	Feature-based transfer learning	C3, C4	EEG
[34]		Feature-based	Common Spatial Patterns (CSP) and LDA	EEG
[24]	BMI decoding	Feature-based transfer learning	Stationary subspace CSP (ssCSP)	EEG
[38]	Variational Bayesian multimodal	Feature-based transfer learning	Principal component analysis (PCA) based CSP	EEG
[43]	Homogenous TL	Parameter‐ based transfer learning	Extreme learning machine (ELM)	EEG

[44]		Parameter‐based transfer learning	Domain adaptation SVM (DASVM)	EEG
Proposed method	Homogenous TL	Feature-based TL	Convolutional Neural Network	fNIRS

5.5 Results

The obtained results after experimentation and statistical analysis are presented in this section. For framework 1, the trained CNN is used for training on the control group. Figure 1 shows the accuracies of control group subjects with training epochs. Fig 3 shows the accuracies of baseline group subjects that are trained on the randomly initialized CNN network. Tables 1 and 2 represent the accuracies of the control group and the baseline group, respectively. The network is trained up to 60 epochs before it starts overfitting.

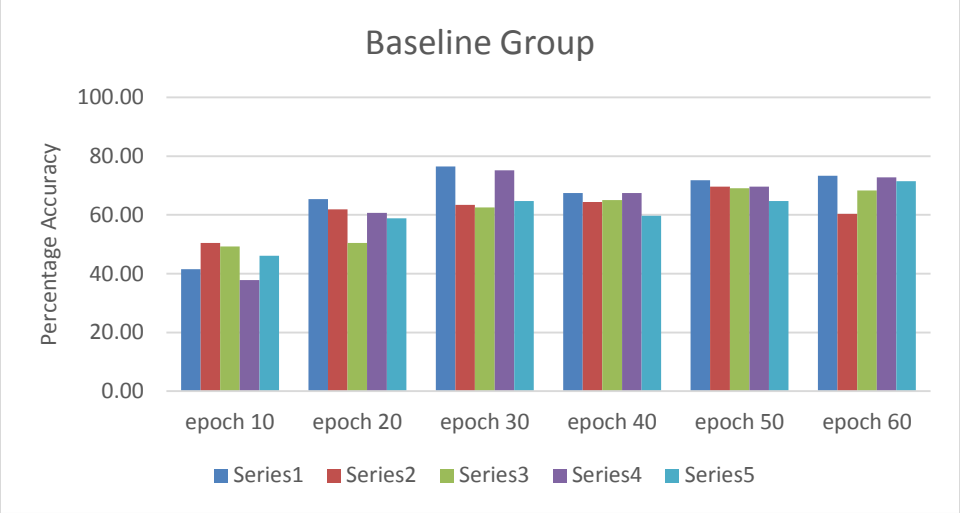

Figure 5-7: Percentage accuracy for baseline group for all series

In this study, we explored the feature-based transfer learning method for the classification of BCI commands to reduce the training and calibration time. In the first approach, we used 16 subjects to train the CNN network, namely learned CNN network, and learn the source domain knowledge of the n-back dataset. Further, we split the remaining 10 subjects into two groups i.e control and baseline. We then train the control group with the learned CNN network and baseline with randomly initialized CNN network and compared their accuracies using statistical analysis. The results suggested that applying the proposed feature-based transfer learning algorithms could

lead to achieving the maximum saturated accuracy 20 epochs sooner than the baseline group which in turn reduces the training time. The proposed transfer learning method also outperformed the averaged accuracy achieved using the learned CNN model over the traditional CNN model by 12%. In the second experiment, we proved that instance-based transfer learning can significantly reduce the calibration time with reasonable accuracy on the 10:90 train-test ratio and become saturate on the 30:70 train-test split ratio of the dataset.

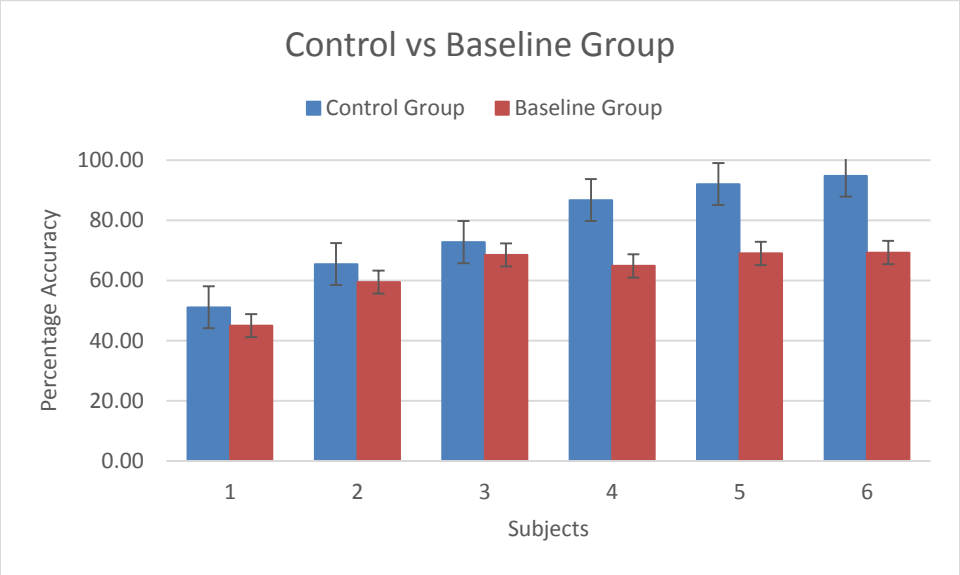

Figure 5-8: Comparison of percentage accuracies between control and baseline group for subjects

5.6 Discussion

The transfer learning algorithms of EEG-based BCI are based mostly on either the importance sampling cross-validation method [26] [27], or the instance selection method [28][29]. In [26], Covariance Shift adaptation or CSA is proposed, in which the target domain's data (other subjects) is weighted on the base of the importance sampling cross-validation method. After that, the estimation of the final prediction function is based on parts that have high weights. An instance selection method is proposed [28][29] on an active learning base to identify the trials, that were found close to few informative trials of new subjects. The trials that were selected were then added to existing labeled trials of a new subject for the BCI model's training (final prediction function). In [30], the deep learning algorithms as the feature extractor in combination with the transfer learning is proposed to diagnose the predisposition to alcoholism. In the feature domain, most of the proposed algorithms of transfer learning focus on the improvement of the common spatial pattern (CSP) by either modifying the covariance matrix estimation method

[31][32], or the common spatial pattern optimization function [22][33]. For example; in [32], the author proposed the extension of common spatial patterns, in which instead of the discriminative information, the stationary information was transferred across the multiple subjects by learning a stationary subspace. In [34], the authors proposed the combination of deep deep-learning-based transfer learning along with Continuous Wavelet Transform (CWT) to solve Motor imagery (MI) for the Brain-Computer Interface. Ensemble learning of the classifiers [20][21] and various domain adaptation techniques [35][36][37] have been adopted for many existing Motor Imagery based. I have explored the feature-based transfer learning method for the classification of BCI commands to reduce the training and calibration time. In the first approach, we used 16 subjects to train the CNN network, namely learned CNN network, and learn the source domain knowledge of the n-back dataset. Further, we split the remaining 10 subjects into two groups i.e control and baseline. We then train the control group with the learned CNN network and baseline with randomly initialized CNN network and compared their accuracies using statistical analysis. We can achieve the maximum saturated accuracy 20 epochs sooner than the baseline group which in turn reduces the training time. The proposed transfer learning method also outperformed the averaged accuracy achieved using the learned CNN model over the traditional CNN model by 12%. In the second experiment, we proved that instance-based transfer learning can significantly reduce the calibration time with reasonable accuracy on the 10:90 train-test ratio and become saturate on the 30:70 train-test split ratio of the dataset.

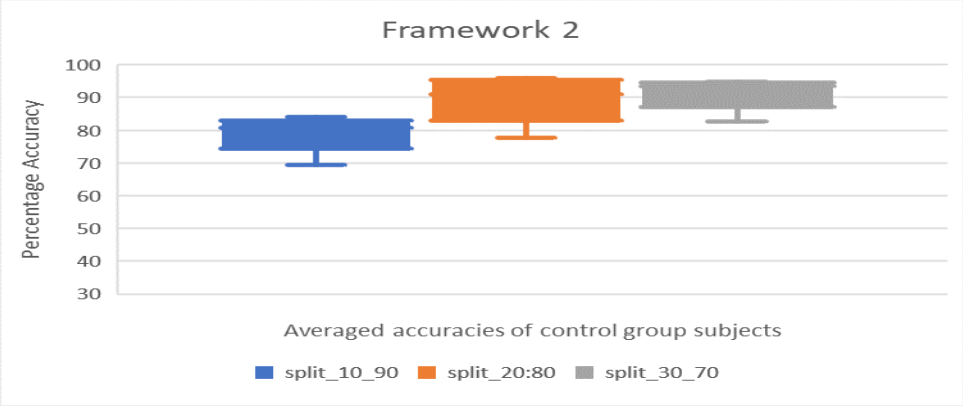

Figure 5-9: Average accuracies of control group subjects

The main objective of Transfer learning (TL) is to produce an effective model [3][6][7] for the target task while tackling the problems of limited labeled training data or no data at all. I have explored the feature-based transfer learning method for the classification of BCI commands to reduce the training and calibration time. In the first approach, we used 16 subjects to train the

CNN network, namely learned CNN network, and learn the source domain knowledge of the n-back dataset. Further, we split the remaining 10 subjects into two groups i.e control and baseline. We then train the control group with the learned CNN network and baseline with randomly initialized CNN network and compared their accuracies using statistical analysis. We can achieve the maximum saturated accuracy 20 epochs sooner than the baseline group which in turn reduces the training time. The proposed transfer learning method also outperformed the averaged accuracy achieved using the learned CNN model over the traditional CNN model by 12%. In the second experiment, we proved that instance-based transfer learning can significantly reduce the calibration time with reasonable accuracy on the 10:90 train-test ratio and become saturate on the 30:70 train-test split ratio of the dataset. It can find some common representative features having same marginal distribution in both domains. The model parameter-based approach of transfer learning uses the source domain's prediction function to improve the prediction function (classifiers) of the target domain.

I have explored the feature-based transfer learning method for the classification of BCI commands to reduce the training and calibration time. In the first approach, we used 16 subjects to train the CNN network, namely learned CNN network, and learn the source domain knowledge of the n-back dataset. Further, we split the remaining 10 subjects into two groups i.e control and baseline. We then train the control group with the learned CNN network and baseline with randomly initialized CNN network and compared their accuracies using statistical analysis. We can achieve the maximum saturated accuracy 20 epochs sooner than the baseline group which in turn reduces the training time. The proposed transfer learning method also outperformed the averaged accuracy achieved using the learned CNN model over the traditional CNN model by 12%. In the second experiment, we proved that instance-based transfer learning can significantly reduce the calibration time with reasonable accuracy on the 10:90 train-test ratio and become saturate on the 30:70 train-test split ratio of the dataset.

CHAPTER 6: MENTAL WORKLOAD APPLIED TO BCI

Mental workload, a Neuroergonomics human factor, is widely used not only in the planning system's safety but also in the areas like brain-machine interface (BMI), neurofeedback, and assistive technologies. Robotic prosthetics methodologies are employed for assisting hemiplegic patients while performing tasks in daily routine activities. The design and operation of assistive technologies require an easy interface with a brain with fewer protocols while trying to optimize mobility and autonomy. The possible answer to these design questions may lie in Neuroergonomics coupled with BMI systems. In this study, two tine human factors are addressed simultaneously; one by designing a lightweight (servo tendon is driven) wearable robotic exoskeleton hand, that is used to assist the stroke patients with an integrated brain interface using a mental workload (MWL) acquired with portable fNIRS system. The system used to generate command signals for operating wearable robotic exoskeleton hand using based two-state MWL signals. The fNIRS is used to record optical signals in form of a change in concentration of oxy and deoxygenated hemoglobin (HbO and HbR) from the prefrontal cortex (PFC) region of the brain. Fifteen participants participated in this study and were given grasping tasks. Two-state MWL signals acquired from the PFC of participants are segregated using support vector machines (SVM) to further utilize in operating robotic exoskeleton hands.

Patients, being suffered from a stroke, need proper training to overcome the deprivation from motor movements. Multiple robotic prostheses have been developed which are giving assistance in daily routine activities to these hemiplegic patients. The ease of use and operation of these assistive technologies remains an issue and how these designed technologies will be giving an easy interface to affected people? The possible answer is a BCI system. In this paper, we have presented a lightweight servo tendon-driven wearable robotic exoskeleton hand which will assist the person being suffered from stroke integrated with an easy interfacing technology for stroke patients i.e., two commands asynchronous Steady-State Visually Evoked Potentials (SSVEP). We designed a monochromatic green light asynchronous SSVEP source board which is being used as a stimuli generator, integrated with a robotic hand. 9 Hz and 10 Hz frequencies have been used in two commands BCI system which are from the alpha band. Emotive Lite-NIRS neuro imagining system is used to record fNIRS signals in form of oxy and deoxygenated hemoglobin. These hemodynamic signals are used to measure the fatigue of the participant with

time. 13 participants took part in this study, 10 right-handed and 3 left-handed mean age =21.73 years ± SD=1.15, participated in this study, maximum accuracy achieved is 95 % and minimum accuracy achieved is 75 %. These results show the feasibility of two commands asynchronous SSVEP based servo tendon driven wearable robotic exoskeleton hand (BCI system) for hemiplegic patients for physical grasping tasks.

Tetraplegia and Stroke are few among the major causes in which a person is not able to fully control his own muscular movements [94]. The Patients suffering from such diseases show uncontrolled motor movements during the early stages and in the later stages, these patients are unable to control their motor movements due to neuronal degeneration [43], [95]. During extreme stages of these diseases, a patient may completely become paralyzed and the person suffering may not be able to perform any daily routine tasks. In the context of injuries, the spinal cord and some brain injuries also contribute to motor disabilities. For such persons, there is a need to devise a methodology by which these patients can be rehabilitated partially if not fully [96]. Brain-Computer Interface (BCI) is among such methods that can provide rehabilitation and assistance to patients with severe motor disabilities. A BCI translates the neuronal or hemodynamic signals that are acquired directly from a patient's brain into useful machine commands that can be used to control devices for the assistance of motor disabled patients. "There are multiple devices that can be used to design a BCI system. Based on portability, low cost, non-invasiveness, electroencephalography (EEG) and functional near-infrared spectroscopy (fNIRS) are the two most widely used modalities for the rehabilitation of a patient" [13], [14]. In comparison to fNIRS, EEG has got a better temporal resolution [15], [16] therefore mostly EEG is used for rehabilitation purposes. BCI based application is now very powerful. The power of imagination can also be considered. Abiri et. al. [39] presented a work in which the scalp EEG was recorded in which the user was imagining different body kinematics while [40] has presented different communication types available in BCI. This imagined body kinematics were decoded using regression model and them mapped on a social robot. Steady State Visual Evoked Potentials (SSVEP) and P300 signals for BCI are usually generated using a visual stimulus. The signal acquisition time of these signals also plays a vital role in control of an external device using a BCI. An SSVEP-based BCI can either be synchronous or asynchronous. If it is synchronous, then the user must know the exact instant at which he/she has to pay attention towards flickering stimulus and if it is asynchronous, then the user is free from this constraint

[44]. Source of SSVEP, frequency, and the number of available choices in SSVEP are important factors that are associated with the Information Transfer Rate (ITR) of a BCI system. Wu. et al. [97] has presented the analysis of three different types of stimulators. The color and luminosity of the source of the SSVEP also matter. Floriano et al. [98] have elaborated the effect of color and luminous and reported that green-red color stimuli are batter in the medium frequency range and green-blue color stimuli are better in the high-frequency range. Diez. et al. and Li. J et al. [99], [100] have presented the utilization of high frequencies in SSVEP and steerability control of wheelchair-using human thoughts. Herrmann et al. have also studied the suitability of different frequencies for SSVEP [101]. According to their findings, 10 Hz, 20 Hz, 40 Hz, and 80 Hz are those frequencies where SSVEP's resonance has been observed. Another study, presented in [102], tried to measure the suitable frequency for SSVEP. They tried to derive a relation between the amplitude of SSVEP as a function of frequency. Though the selection of frequency for SSVEP is an important thing but the harmonics consideration is also important. Muller-Putz et al. [103] have reported that the inclusion of three harmonics increases the classification accuracy in four class BCI systems. Abiri et al. [104] have presented a review of different types of paradigms that have been presented in different types of BCI systems. The number of commands also decides the number of possibilities, speed of communication, and accuracy of a BCI system. It is not necessary that the environment, where the SSVEP signals are being taken, is fully calm or it might possible that the person, using SSVEP, is not fully calm. Chaudhary et al. [40] have studied the effect of deliberately introduced perturbations while using SSVEP. Introduced perturbations were speaking, listening, and thinking while EEG is being recorded. Results showed that speaking and thinking affect the classification accuracy while listening does not affect much.

A BCI system mainly comprises different parts, among these parts, Signal processing, and feature extraction are the most important ones. Ortiz et al. and Volosyak et al. [41], [42] have presented a review of non-invasive EEG signal processing techniques for SSVEP based applications, and [43] has presented a comprehensive study of different useful features in fNIRS-EEG based activities. Multiple types of noise are present in EEG including different artifacts as well. Xie. et al. [50] has studied the effect of spatiotemporal visual noise on the compensation of mental load and fatigue and [51] has given the inclusion of fuzzy control in this field. It is important to have a proper mechanism along with brain signals to ensure a proper control for

BCI. Erkan et al. [44], has reported that minimum energy combination (MEC) and canonical correlation analysis (CCA) can be used in the detection of SSVEP signals in EEG recording but MEC is recommended for synchronous SSVEP stimulus. Gao. et al. [45] showed the feasibility of the SSVEP using an electric apparatus. The patient is introduced to different flickering lights (boxes) which flashes at different rates and represent different actions against each (chosen from a menu). Along with brain signals, a prober haptic/ prosthetic device is needed for the patient to perform daily routines. Researches mostly focus on the design of the BCI technique while ignoring the design parameters of the haptic device. The recorded and processed brain signals can drive different mobile robots which are acting as social/assistive robots ensuring that the person is not in a drowsiness state [2]. A comprehensive survey of these mobile robots has been presented in [83]. Among all mobile robots, a wheelchair is most prominent and the role of these mobile robots in the life of people suffering from a disability is also stated in [99], [105] in which different researchers have presented different types of application of SSVEP. A comprehensive review of different types of wheelchairs along with their driving and classification mechanisms is presented in [106], [107]. Zhang et al. [108] have given an algorithm for the detection of idle state in SSVEP based BCI applications which have also been used in a wheelchair.

In this research, we present a novel fNIRS based lightweight servo tendon driven wearable exoskeleton hand mechanism for hemiplegic patients (performing daily routine tasks). Unlike previous researches, our designed wearable exoskeleton has separately controllable five fingers and improved accuracy. We used 12 channels fNIRS system for data acquisition recording [39]. The system acquired fNIRS signals and measured the two levels of mental workload (MWL). A total of 15 subjects participated in this study. Primarily two features from the hemodynamic signals namely mean and slope were extracted and employed SVM classifier, the maximum accuracy is 98.30%, with the average accuracy is 93.97%. The system is summarized in the figure below.

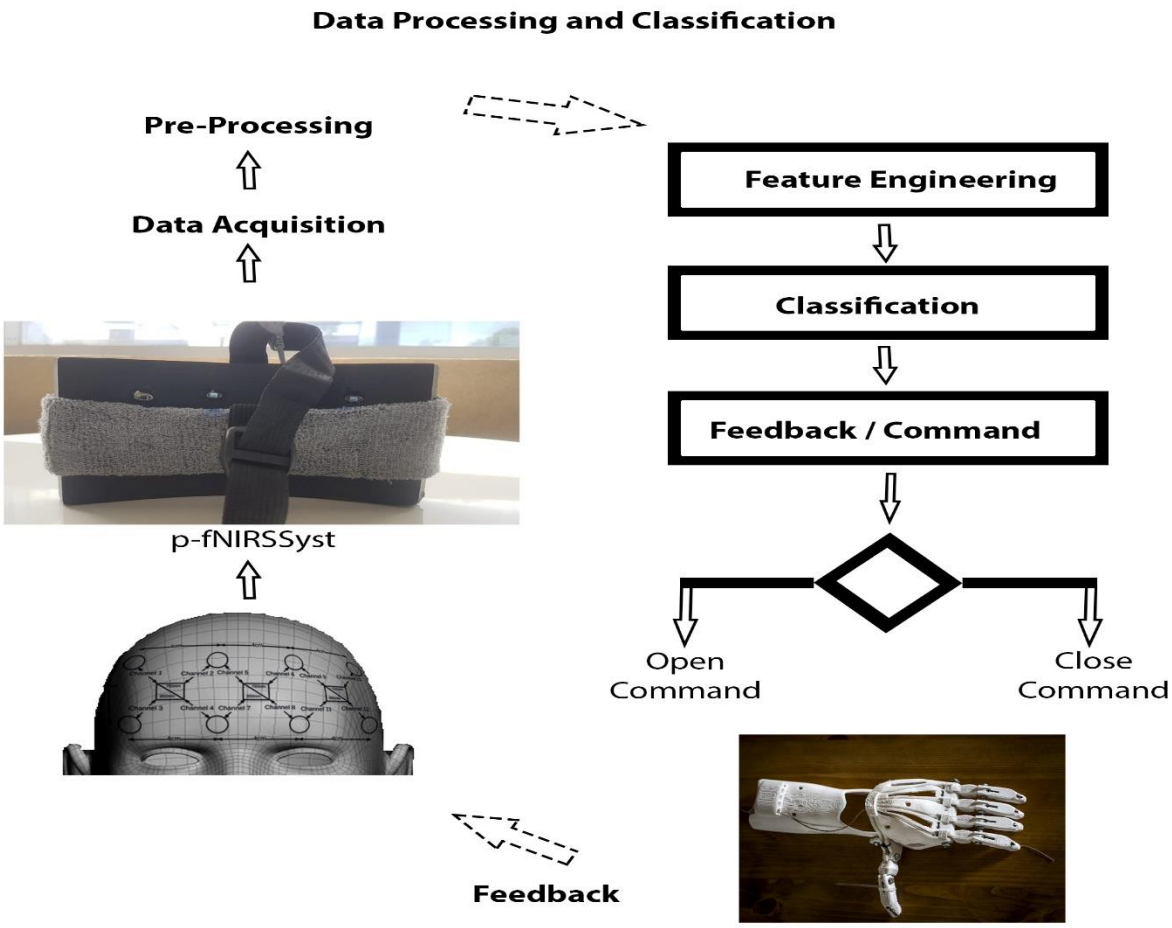

Figure 6-1: Data processing and classification system

6.1 Experimental protocol

The whole architecture is presented in Figure 5. The subject with the robotic hand wears the fNIRS device on the scalp which is continuously measuring hemodynamic concentration changes in the prefrontal cortex as shown in Figure 5. The subject must concentrate on mental math for a few seconds and then fNIRS signals will be taken from the fNIRS headset and processed in the benchmark study [39]. A total of 15 healthy subjects (12 male, 3 female, and all right-handed) have participated in this study and all of them were teenagers.

fNIRS signal recording duration is 20 seconds and then some preprocessing has been done. The experiment was designed to discriminate between two MWL levels. The participants sit in a dimly lighted area with back seats against a 17-inch monitor and were advised to avoid any unnecessary physical motion. They were presented with slides to give experiment details and

procedures before anything else. The initial 146 seconds were a rest period to set the baseline. The baseline period is followed by MWL level 1 in which subjects performed mental arithmetic tasks for 20 seconds and 20 seconds rest periods. Targeting the most affected patients of stroke, we have devised two commands asynchronous SSVEP based servo tendon driven exoskeleton hand for grasping task. Targeting the most affected patients of stroke, we have devised two commands fNIRS based servo tendon driven exoskeleton hand for grasping task. The two-level of the mental workload are recorded with the fNIRS device at 8 Hz sampling frequency. The maximum accuracy achieved is 91.31% while the minimum averaged accuracy is 80.15%. Targeted channels are PF1, PF2, and PFz. After normalizing channel readings, we used the 4^{th} order low-passed Butterworth bandpass. Then we used SVM to generate a command (either open or close) for a prosthetic hand. Results showed the effectiveness of the used technique for those suffering from a severe level of strokes. Accumulated Power Spectral Density (PSD) is used along with CCA and frequency contents of the filtered signal have been extracted. Results showed the validity of the used technique to those suffering from severe levels of strokes The same procedure is repeated for 10 trials. MWL level 1 consists of simple three number addition tasks such as 349 + 547, 564 + 986 etc. MWL level 1 was modeled such that it induces a minimal amount of MWL [109]. After 10 trials of MWL level 1, subjects are presented with MWL level 2 with a delay of 25 seconds. The MWL level 2 also follows the same pattern of 20 seconds activity and 20 seconds rest with a total of 10 trials. The MWL level 2 contains arithmetic operations on equations and their answers (ANS) being utilized in the next calculation (e.g. 768 – 5, ANS x 4, ANS – 32, ANS + 912). MWL level 2 involves mental arithmetic tasks, short term memory, and mental math [110], [111]. The difficulty level of MWL level 2 is greater than that of MWL level 1 and induces more MWL.

These processed signals are translated into two commands, i.e., “open” and “close” and then fed into the robotic hand as shown in Figure 6. The experimental settings are designed to differentiate into two levels of mental workload. In previous studies, mental arithmetic and programming tasks are also used to provoke the brain and create a certain amount of mental workload [112], [113] and can be used to generate discriminative signals to BMI systems.

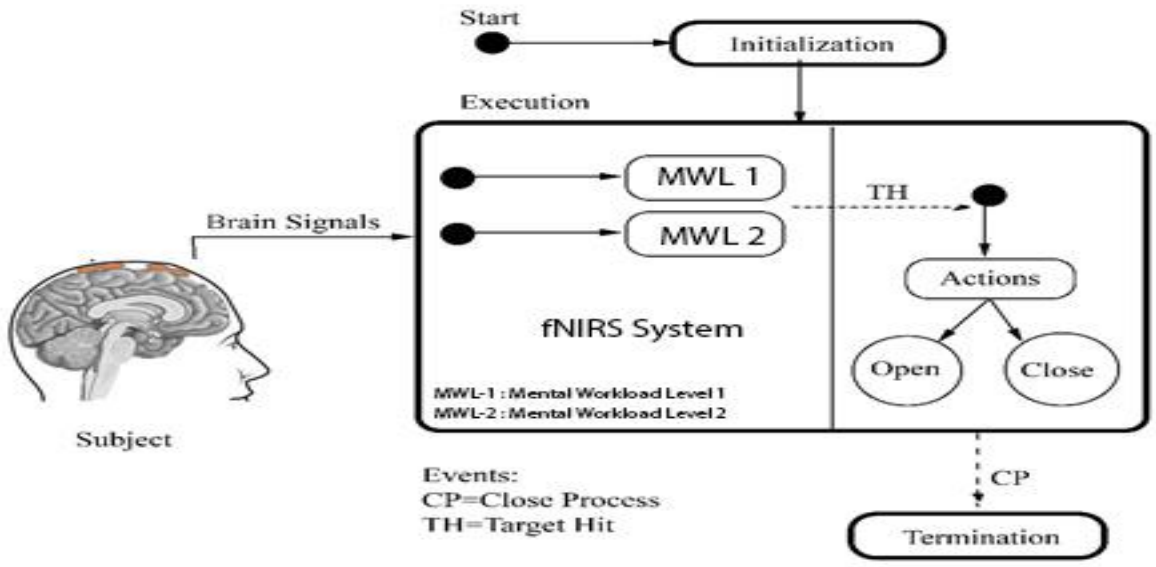

Figure 6-2: Experiment protocol for practical BCI

We used the P-fNIRSSyst headset for the acquisition of brain signals. Targeted channels are PF1, PF2, and PFz of the pre-frontal cortex region [75].

6.2 Information Transfer Rate

Information Transfer Rate (ITR) is an assessment metric broadly employed in BCI systems to estimate the amount of information in bits passed-on by the system's output [114]. This is a recognized statistic that mental tasks decreases the reliability of classification accuracy. ITR, first introduced in information theory, is used to quantify this reliability [115]. It is denoted by B and is calculated by eq (1)

$$B = log_2 N + P\, log_2 (P) + (1 - P) log_2 \frac{1-P}{N-1} \qquad \text{eq (2)}$$

Where N is the classification tasks and P is the obtained classification accuracy.

The temporal resolution of fNIRS usually depends on the properties of the underlying evoked neuronal and vascular changes. The time series plot of blood oxygenated level-dependent (BOLD) the nature of applied stimuli and hemodynamic response to neuronal events and is called hemodynamic response function (HRF). The standard HRF shows the signal peaks during 5-8 sec after triggering neuronal events because neuronal activity increases metabolic demands that lead to an increase in the influx of oxygenated blood. Since the inflow of oxygenated blood

continues and results in more supply than demand, the HRF becomes straightened roughly after 10 sec [4], [17]. The hrf for this study is calculated by spatially averaging across all channels and then temporally averaging the obtained vector from the previous step concerning the number of trials i.e. 10 for each MWL. A total of 16 subjects (eleven male and five female) initially participated, in this study with age ranging from 20 to 27 years, mean age of 23.5 years, and a standard deviation of 5.5 years. Medical screening is performed under the supervision of a doctor to assess any physical or psychological issues in the participants. Participants were given the details about the experiment before the experimentation. The fNIRS recording of one subject was more than 10% contaminated with channel noise and was excluded from further analysis. The remaining fifteen subjects (ten male and five female) data was analyzed.

Table 6-1: Hand open, hand close and average accuracies of subjects

Subjects	Total commands of each category	Open Success	Close Success	Hand open accuracy	Hand close accuracy	Average accuracy
Part 1	10	8	9	80.00	90.00	85.00
Part 2	-do-	9	8	90.00	80.00	85.00
Part 3	-do-	9	8	90.00	80.00	85.00
Part 4	-do-	8	7	80.00	70.00	75.00
Part 5	-do-	9	9	90.00	90.00	90.00
Part 6	-do-	10	9	100.00	90.00	95.00
Part 7	-do-	8	8	80.00	80.00	80.00
Part 8	-do-	7	9	70.00	90.00	80.00
Part 9	-do-	8	7	80.00	70.00	75.00
Part 10	-do-	9	8	90.00	80.00	85.00
Part 11	-do-	8	8	80.00	80.00	80.00
Part 12	-do-	7	9	70.00	90.00	80.00
Part 13	-do-	9	8	90.00	80.00	85.00
Average	**10**	**8.38**	**8.23**	**83.84**	**82.30**	**83.07**

The total length of the recorded signal is 4 seconds. Maximum accuracy achieved is 95% while the minimum accuracy achieved is 75%. PSD plots of different acquired EEG signals and, controlling commands, after preprocessing, signals are shown along with the corresponding opening and closing angles of the hand's MIP and DIP joints data and implementation on exoskeleton hand.

Table 4-2: Subject gender, age and dominan hand details

Subjects	**Gender**	**Age (Years)**	**Glasses**	**Writing hand**
Part 1	Male	21	NO	Right
Part 2	-do-	22	NO	-do-
Part 3	-do-	22.5	NO	-do-
Part 4	-do-	24	NO	Left
Part 5	-do-	23	YES	Right
Part 6	-do-	22	NO	-do-
Part 7	-do-	21.5	NO	-do-
Part 8	-do-	22	NO	-do-
Part 9	-do-	20	NO	Left
Part 10	-do-	21.5	NO	Right
Part 11	Female	19.6	YES	Left
Part 12	-do-	21.4	NO	Right
Part 13	-do-	22.1	NO	-do-
Average	***	**21.73±1.15**	***	***

6.3 Results

c

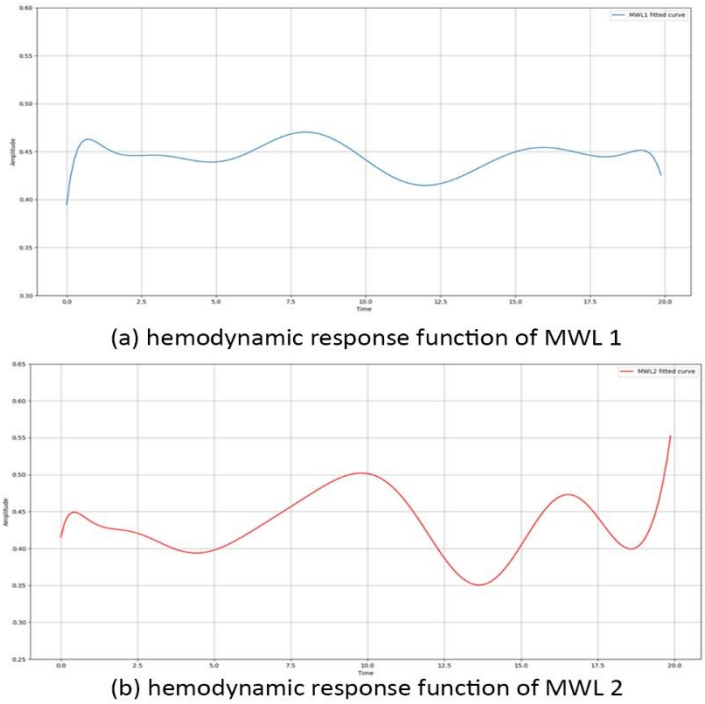

Figure 6-3: Hemodynamic response function of MWL 1 and 2

Targeting the most affected patients of stroke, we have devised two commands asynchronous SSVEP based servo tendon driven exoskeleton hand for grasping task. Targeting the most affected patients of stroke, we have devised two commands fNIRS based servo tendon driven exoskeleton hand for grasping task. The two-level of the mental workload are recorded with the fNIRS device at 8 Hz sampling frequency. The maximum accuracy achieved is 91.31% while the minimum averaged accuracy is 80.15%. Targeted channels are PF1, PF2, and PFz. After normalizing channel readings, we used the 4^{th} order low-passed Butterworth bandpass. Then we used SVM to generate a command (either open or close) for a prosthetic hand. Results showed the effectiveness of the used technique for those suffering from a severe level of strokes. Accumulated Power Spectral Density (PSD) is used along with CCA and frequency contents of the filtered signal have been extracted. Results showed the validity of the used technique to those suffering from severe levels of strokes.

CHAPTER 7: CONCLUSIONS AND FUTURE WORK

In the first part of this study, a detailed analysis of human behavior and memory activities in the brain using different machine learning (ML) and deep learning (DL) classification algorithms is performed. The next part includes the comparison between the computational requirement of different ML and DL algorithms for analyzing human behavior and memory activities in the brain for a brain-machine interface. Further in the line, the fast and efficient heartbeat classification algorithm is presented, and then the novel application of mental workload in soft exoskeleton (servo motor driven) fNIRS-based brain-computer interface (BCI) system is discussed. Lastly, the novel symmetric based homogenous transfer learning is applied on fNIRS data to reduce calibration and training time. Targeting the most affected patients of stroke, we have devised two commands mental workload based servo tendon driven exoskeleton hand for grasping task. Targeting the most affected patients of stroke, I have devised two commands fNIRS based servo tendon driven exoskeleton hand for grasping task. The results confirm the possibility of utilizing mental workload as an application for brain-computer interfacing. Previously, different studies have utilized synchronous and asynchronous SSVEP, motor and imagery activity to drive the exoskeleton.

The recurrent neural network has an excellent ability of pattern recognition in sequences of input. But they have stability issues either due to exploding gradients or vanishing gradients. I used a variant of recurrent neural network that solved the exploding and vanishing gradient problem by using memory cells. By exploiting that variant namely Long Short Term Memory (LSTM), the highest classification accuracy of four class mental workload data for the brain-computer interface is achieved. This is indeed a state of the art algorithm in the present brain-computer interface realm. The heartbeat classification has paramount importance in detecting cardiovascular diseases. The ultra-low-powered classifier with state of the art accuracy is presented in this dissertation. The classifier is based on an extreme learning machine (ELM) algorithm. The ELMs do not require gradient descent and backpropagation for training. This makes them an excellent choice as they do not require a long time for training. Also, they have in order of magnitude fewer parameters than artificial neural networks and convolutional neural networks.

The comparison between the proposed extreme learning machines algorithm with another state of the art algorithms are presented and it turns out that, besides being fewer parameters and very fast training time, our method compete toe-to-toe with the other gradient descent and backpropagation based algorithms. Extending the same theme, in the next study, the resource comparison between machine learning and deep learning algorithms is performed. The deep learning algorithms, thanks to their auto feature extraction ability, are getting more and more popular these days. But this comes at the cost of longer training time, more computer resources, and the requirement of an ample amount of training dataset. This study was designed to evaluate both ml and dl algorithms in light of the above-mentioned nuances. Deep Learning (DL) for such classification purposes due to feature engineering and complex data pre-processing requirements of machine learning algorithms.

Bypassing the challenges of feature engineering through DL techniques comes at the cost of time and computational complexity of the system. I utilize the neuroimaging recordings and perform MWL classification using conventional LDA, k-NN, SVM, and DL algorithms ANN, CNN, and a recurrent neural network LSTM. In this study, we discussed the theoretical computational complexities and compared generalizability, classification accuracies, train and test time requirements of k-NN, SVM, ANN, CNN, and LSTM. The averaged accuracy achieved using k-NN, SVM, ANN, CNN, and LSTM is 92.54, 81.47, 64.80, 55.94, 58.61, and 32.13 % while averaged train time being 127.40, 7.57, 1.41, 0.45, 0.01, and 0.03 sec and test time being 0.603, 0.040, 0.038, 0.039, 0.061, and 0.00032 sec, respectively. The findings suggest that ML algorithms are recommended for real-time BCI with low commands and focus on efficient computation while DL algorithms are recommended for use cases where high commands and accuracy are of prime importance. CNN covers the nice ground between optimal classification accuracy and reasonable train, the test time. In the light of these findings, I present an alternative solution to solve the deep learning algorithms shortcoming. I explored the feature-based transfer learning method for the classification of BCI commands to reduce the training and calibration time. In the first approach, we used 16 subjects to train the CNN network, namely learned CNN network, and learn the source domain knowledge of the n-back dataset. Further, we split the remaining 10 subjects into two groups i.e control and baseline. We then train the control group with the learned CNN network and baseline with randomly initialized CNN network and compared their accuracies using statistical analysis. We can achieve the maximum saturated

accuracy 20 epochs sooner than the baseline group which in turn reduces the training time. The proposed transfer learning method also outperformed the averaged accuracy achieved using the learned CNN model over the traditional CNN model by 12%. In the second experiment, we proved that instance-based transfer learning can significantly reduce the calibration time with reasonable accuracy on the 10:90 train-test ratio and become saturate on the 30:70 train-test split ratio of the dataset.

The fNIRS based BCI took substantially more time to generate commands than EEG, there is a lot of room to work on early activity detection. RNN based BCI is a new class of algorithm for brain signal classification. There is a need for a lot of experimentation for RNN variants, especially GRUs, having fewer parameters than LSTM, which can be one possible direction. There are a lot of potential applications for asymmetric homogenous transfer learning. Working in that direction will help researchers to mitigate nuances attached to deep learning algorithms.

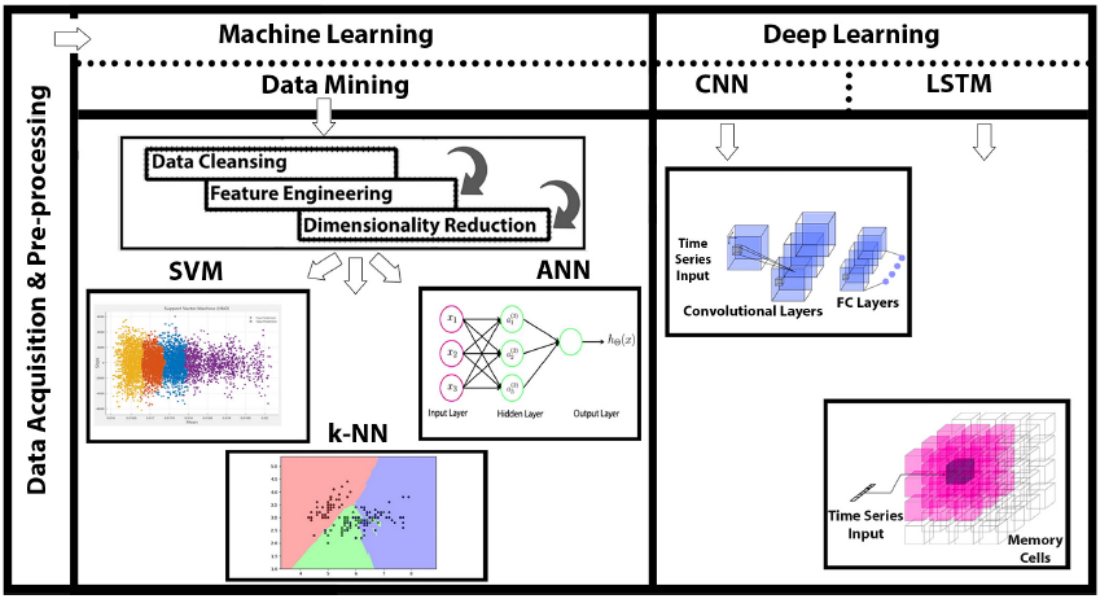

FIGURE 1 | Functional near-infrared spectroscopy (fNIRS)-based mental workload (MWL) classification using machine learning (ML) and deep learning (DL) algorithms. Data acquisition through fNIRS system (P-fNIRSSyst), data preprocessing, and detailed feature engineering followed with application of ML and DL classification.

FIGURE 2 | The functional near-infrared spectroscopy (fNIRS) (P-fNIRSSyst) system placed to measure participants' prefrontal cortex (PFC) activity. Optodes are placed according to the standard 10–20 system.

APPENDIX A

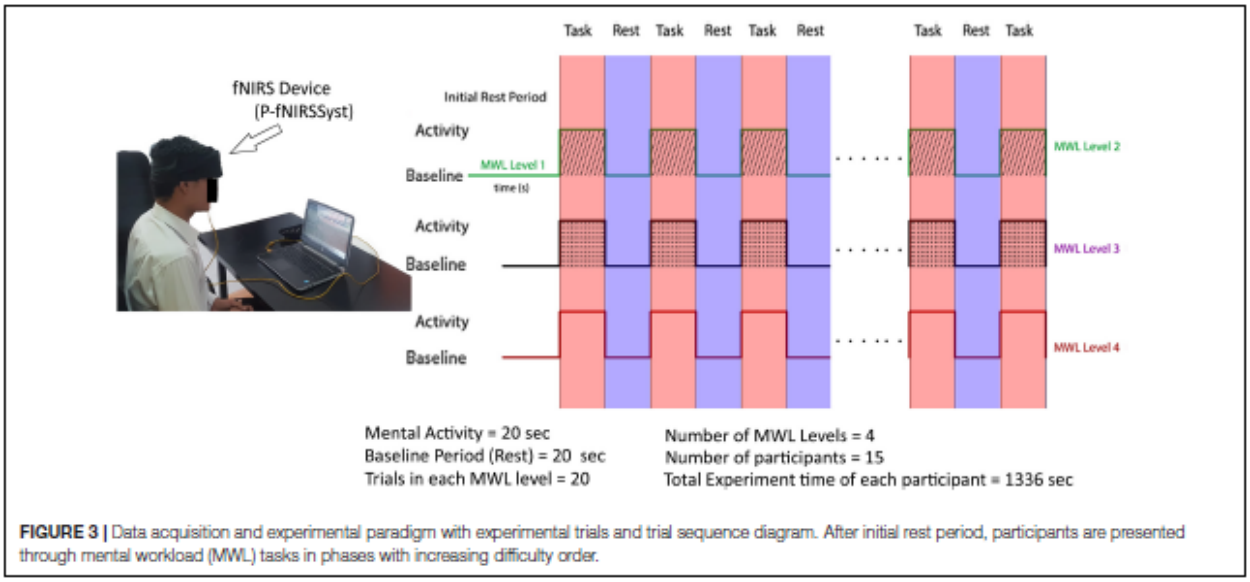

FIGURE 3 | Data acquisition and experimental paradigm with experimental trials and trial sequence diagram. After initial rest period, participants are presented through mental workload (MWL) tasks in phases with increasing difficulty order.

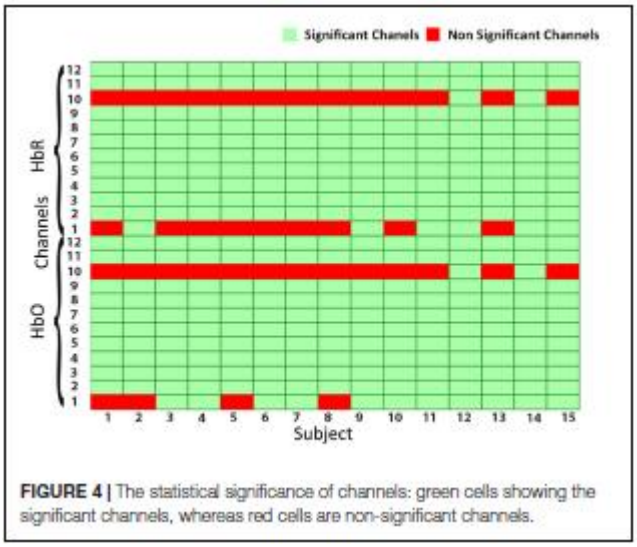

FIGURE 4 | The statistical significance of channels: green cells showing the significant channels, whereas red cells are non-significant channels.

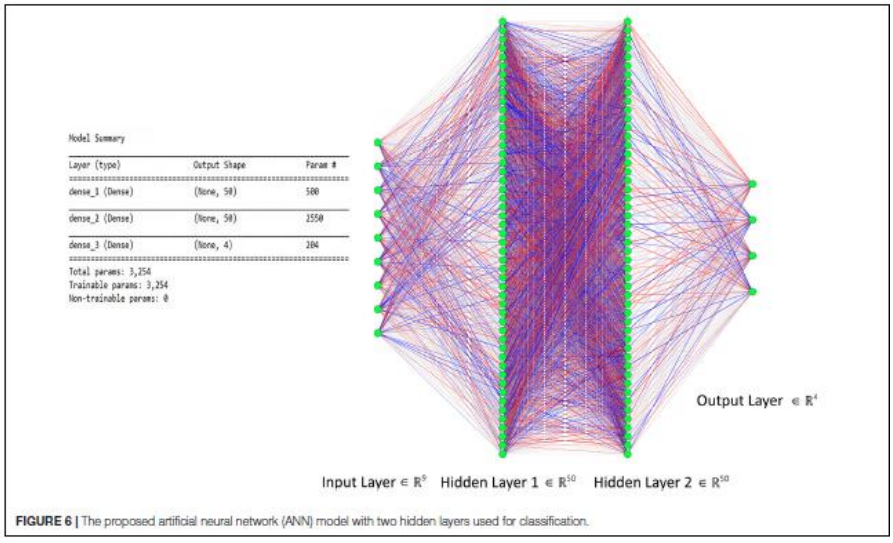

FIGURE 6 | The proposed artificial neural network (ANN) model with two hidden layers used for classification.

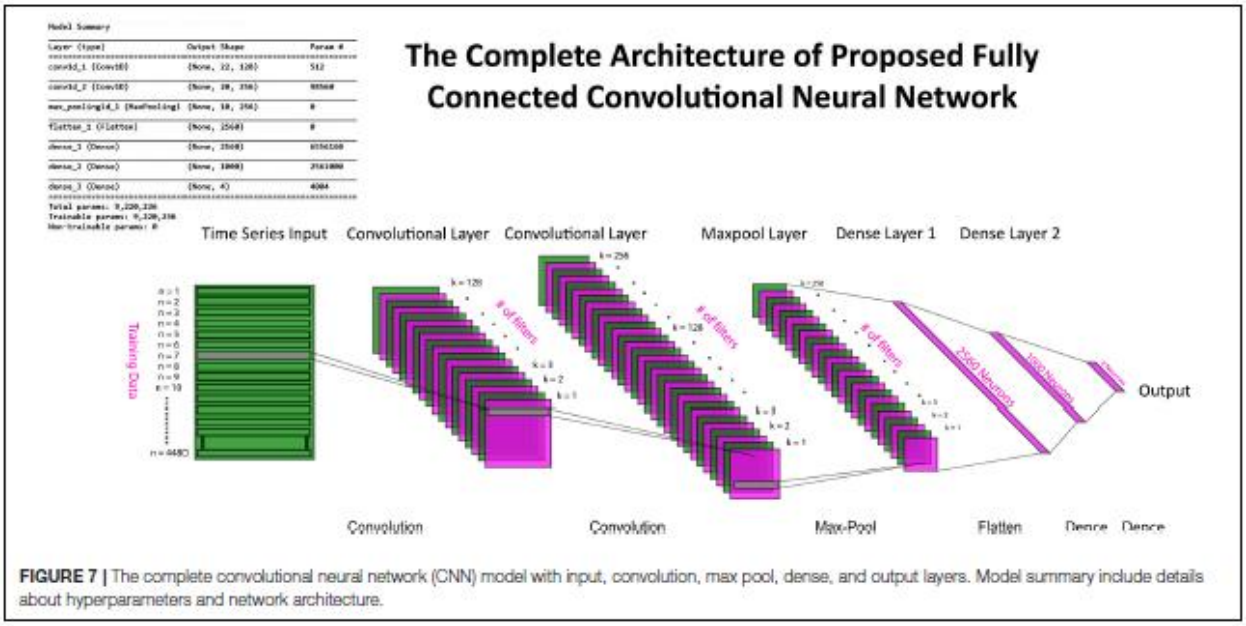

FIGURE 7 | The complete convolutional neural network (CNN) model with input, convolution, max pool, dense, and output layers. Model summary include details about hyperparameters and network architecture.

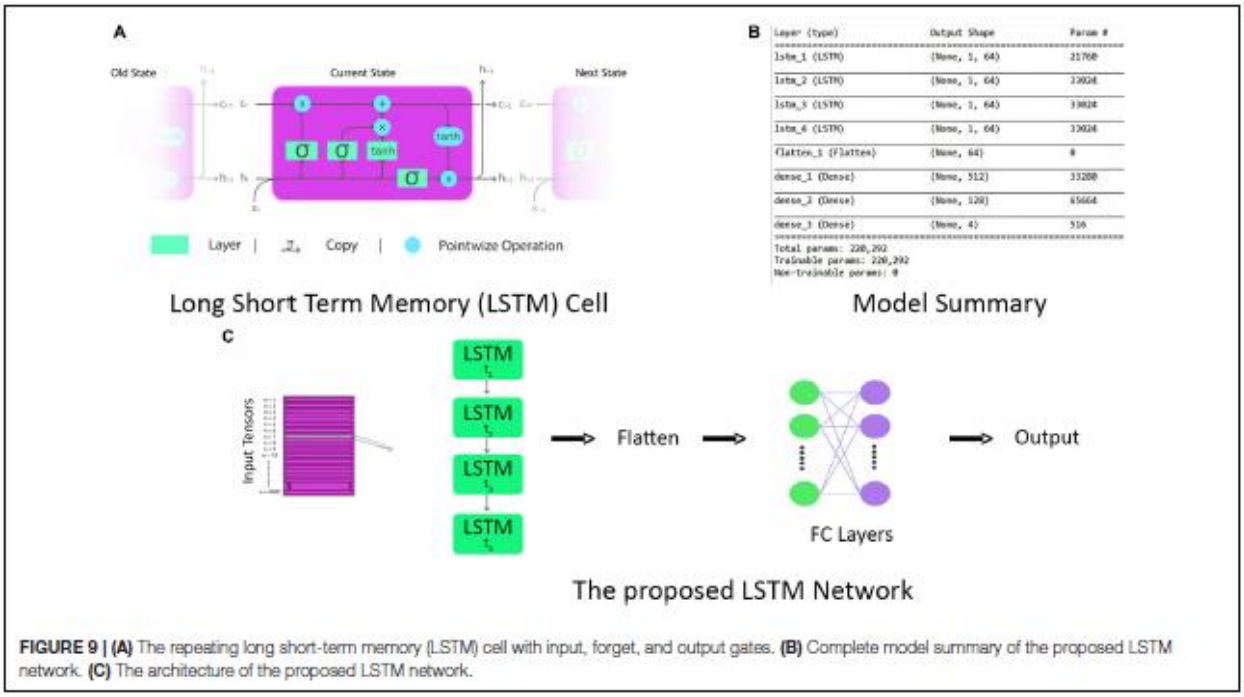

FIGURE 9 | (A) The repeating long short-term memory (LSTM) cell with input, forget, and output gates. **(B)** Complete model summary of the proposed LSTM network. **(C)** The architecture of the proposed LSTM network.

REFERENCES

[1] K. D. Tanner, "Issues in neuroscience education: Making connections," *CBE Life Sciences Education*, 2006.

[2] M. J. Khan and K.-S. Hong, "Passive BCI based on drowsiness detection: an fNIRS study," *Biomed. Opt. Express*, 2015.

[3] M. A. Tanveer, M. J. Khan, M. J. Qureshi, N. Naseer, and K.-S. Hong, "Enhanced Drowsiness Detection Using Deep Learning: An fNIRS Study," *IEEE Access*, 2019.

[4] K. S. Hong and M. J. Khan, "Hybrid brain-computer interface techniques for improved classification accuracy and increased number of commands: A review," *Frontiers in Neurorobotics*. 2017.

[5] "Human Factors," *Intell. Veh.*, pp. 345–394, Jan. 2018.

[6] A. Byrne, "Mental workload as a key factor in clinical decision making," *Adv. Heal. Sci. Educ.*, 2013.

[7] S. Bioulac *et al.*, "Risk of motor vehicle accidents related to sleepiness at the wheel: A systematic review and meta-analysis," *Sleep*. 2017.

[8] M. Saadati, J. Nelson, and H. Ayaz, "Convolutional Neural Network for Hybrid fNIRS-EEG Mental Workload Classification," in *International Conference on Applied Human Factors and Ergonomics*, 2019, pp. 221–232.

[9] J. M. Noyes and D. P. J. Bruneau, "A self-analysis of the NASA-TLX workload measure," *Ergonomics*, 2007.

[10] S. Paulhus, D.L., Vazire, "The Self-Report Method," *Handb. Res. methods Personal. Psychol.*, 2005.

[11] B. Cain, "A Review of the Mental Workload Literature," *Def. Res. Dev. Toronto*, 2007.

[12] T. Q. Tran, R. L. Boring, D. D. Dudenhoeffer, B. P. Hallbert, M. D. Keller, and T. M. Anderson, "Advantages and disadvantages of physiological assessment for next generation control room design," in *IEEE Conference on Human Factors and Power Plants*, 2007.

[13] X. Chen, B. Zhao, Y. Wang, S. Xu, and X. Gao, "Control of a 7-DOF Robotic Arm System With an SSVEP-Based BCI," *Int. J. Neural Syst.*, vol. 28 8, p. 1850018, 2018.

[14] S.-I. Choi *et al.*, "On the feasibility of using an ear-eeg to develop an endogenous brain-computer interface," *Sensors*, vol. 18, no. 9, p. 2856, 2018.

[15] M. Ferrari and V. Quaresima, "A brief review on the history of human functional near-infrared spectroscopy (fNIRS) development and fields of application," *Neuroimage*, vol. 63, no. 2, pp. 921–935, 2012.

[16] J. León-Carrión and U. León-Dom\'\inguez, "Functional near-infrared spectroscopy (fNIRS): principles and neuroscientific applications," in *Neuroimaging-Methods*, IntechOpen, 2012.

[17] N. Naseer and K. S. Hong, "fNIRS-based brain-computer interfaces: A review," *Frontiers in Human Neuroscience*. 2015.

[18] M. J. Khan and K.-S. Hong, "hybrid eeg--fnirs-Based eight-command Decoding for Bci: application to Quadcopter control," *Front. Neurorobot.*, vol. 11, p. 6, 2017.

[19] S. Weyand, K. Takehara-Nishiuchi, and T. Chau, "Weaning Off Mental Tasks to Achieve Voluntary Self-Regulatory Control of a Near-Infrared Spectroscopy Brain-Computer Interface," *IEEE Trans. Neural Syst.*

Rehabil. Eng., 2015.

[20] S. Barbosa, G. Pires, and U. Nunes, "Toward a reliable gaze-independent hybrid BCI combining visual and natural auditory stimuli," *J. Neurosci. Methods*, 2016.

[21] Y. Li, G. Zhou, D. Graham, and A. Holtzhauer, "Towards an EEG-based brain-computer interface for online robot control," *Multimed. Tools Appl.*, 2016.

[22] C. Canning and M. Scheutz, "Functional Near-Infrared Spectroscopy in Human-Robot Interaction," *J. Human-Robot Interact.*, 2013.

[23] M. Rehan and K. S. Hong, "Robust synchronization of delayed chaotic FitzHugh-Nagumo neurons under external electrical stimulation," *Comput. Math. Methods Med.*, 2012.

[24] R. A. Khan, N. Naseer, N. K. Qureshi, F. M. Noori, H. Nazeer, and M. U. Khan, "FNIRS-based Neurorobotic Interface for gait rehabilitation," *J. Neuroeng. Rehabil.*, 2018.

[25] R. Holtzer, J. R. Mahoney, M. Izzetoglu, C. Wang, S. England, and J. Verghese, "Online fronto-cortical control of simple and attention-demanding locomotion in humans," *Neuroimage*, 2015.

[26] N. Naseer, M. J. Hong, and K. S. Hong, "Online binary decision decoding using functional near-infrared spectroscopy for the development of brain-computer interface," *Exp. Brain Res.*, 2014.

[27] J. D. R. Millán *et al.*, "Combining brain-computer interfaces and assistive technologies: State-of-the-art and challenges," *Frontiers in Neuroscience*. 2010.

[28] M. Krauledat, M. Schröder, B. Blankertz, and K. R. Müller, "Reducing calibration time for brain-computer interfaces: A clustering approach," in *Advances in Neural Information Processing Systems*, 2007.

[29] X. Zhang, L. Yao, X. Wang, J. Monaghan, and D. Mcalpine, "A Survey on Deep Learning based Brain Computer Interface: Recent Advances and New Frontiers," *arXiv Prepr. arXiv1905.04149*, 2019.

[30] S. Brigadoi *et al.*, "Motion artifacts in functional near-infrared spectroscopy: A comparison of motion correction techniques applied to real cognitive data," *Neuroimage*, 2014.

[31] G. Bauernfeind, S. C. Wriessnegger, I. Daly, and G. R. Müller-Putz, "Separating heart and brain: On the reduction of physiological noise from multichannel functional near-infrared spectroscopy (fNIRS) signals," *J. Neural Eng.*, 2014.

[32] M. Wronkiewicz, E. Larson, and A. K. C. Lee, "Leveraging anatomical information to improve transfer learning in brain-computer interfaces," *J. Neural Eng.*, 2015.

[33] V. Jayaram, M. Alamgir, Y. Altun, B. Scholkopf, and M. Grosse-Wentrup, "Transfer Learning in Brain-Computer Interfaces," *IEEE Comput. Intell. Mag.*, 2016.

[34] T. J. Huppert, S. G. Diamond, M. A. Franceschini, and D. A. Boas, "HomER: A review of time-series analysis methods for near-infrared spectroscopy of the brain," *Appl. Opt.*, 2009.

[35] W. Tu and S. Sun, "A subject transfer framework for EEG classification," *Neurocomputing*, 2012.

[36] S. Fazli, F. Popescu, M. Danóczy, B. Blankertz, K. R. Müller, and C. Grozea, "Subject-independent mental state classification in single trials," *Neural Networks*, 2009.

[37] F. Lotte and C. Guan, "Learning from other subjects helps reducing brain-computer interface calibration time," in *ICASSP, IEEE International Conference on Acoustics, Speech and Signal Processing* -

Proceedings, 2010.

[38] "Handbook of research methods in personality psychology," *Choice Rev. Online*, 2007.

[39] R. Abiri, X. Zhao, G. Heise, Y. Jiang, and F. Abiri, "Brain computer interface for gesture control of a social robot: An offline study," in *Electrical Engineering (ICEE), 2017 Iranian Conference on*, 2017, pp. 113–117.

[40] U. Chaudhary, N. Birbaumer, and A. Ramos-Murguialday, "Brain--computer interfaces for communication and rehabilitation," *Nat. Rev. Neurol.*, vol. 12, no. 9, p. 513, 2016.

[41] A. Ortiz-Rosario and H. Adeli, "Brain-computer interface technologies: from signal to action," *Rev. Neurosci.*, vol. 24, no. 5, pp. 537–552, 2013.

[42] I. Volosyak, "SSVEP-based Bremen--BCI interface—boosting information transfer rates," *J. Neural Eng.*, vol. 8, no. 3, p. 36020, 2011.

[43] K.-S. Hong, M. J. Khan, and M. J. Hong, "Feature extraction and classification methods for hybrid fNIRS-EEG brain-computer interfaces," *Front. Hum. Neurosci.*, vol. 12, 2018.

[44] E. Erkan and M. Akbaba, "A study on performance increasing in SSVEP based BCI application," *Eng. Sci. Technol. an Int. J.*, vol. 21, no. 3, pp. 421–427, 2018.

[45] X. Gao, D. Xu, M. Cheng, and S. Gao, "A BCI-based environmental controller for the motion-disabled," *IEEE Trans. neural Syst. Rehabil. Eng.*, vol. 11, no. 2, pp. 137–140, 2003.

[46] M. Causse, Z. Chua, V. Peysakhovich, N. Del Campo, and N. Matton, "Mental workload and neural efficiency quantified in the prefrontal cortex using fNIRS," *Sci. Rep.*, 2017.

[47] P. H. S. Pelicioni, M. Tijsma, S. R. Lord, and J. Menant, "Prefrontal cortical activation measured by fNIRS during walking: effects of age, disease and secondary task," *PeerJ*, 2019.

[48] F. Al-Shargie, T. B. Tang, and M. Kiguchi, "Stress Assessment Based on Decision Fusion of EEG and fNIRS Signals," *IEEE Access*, 2017.

[49] N. Thanh Hai, N. Q. Cuong, T. Q. Dang Khoa, and V. Van Toi, "Temporal hemodynamic classification of two hands tapping using functional near-infrared spectroscopy," *Front. Hum. Neurosci.*, 2013.

[50] J. Xie *et al.*, "The role of visual noise in influencing mental load and fatigue in a steady-state motion visual evoked potential-based brain-computer Interface," *Sensors*, vol. 17, no. 8, p. 1873, 2017.

[51] Y.-J. Chen, S.-C. Chen, I. Zaeni, and C.-M. Wu, "Fuzzy tracking and control algorithm for an SSVEP-based BCI system," *Appl. Sci.*, vol. 6, no. 10, p. 270, 2016.

[52] S. Mendis, P. Puska, B. Norrving, World Health Organization., World Heart Federation., and World Stroke Organization., "WHO | Global atlas on cardiovascular disease prevention and control," *Who*, 2011.

[53] Centers for Disease Control and Prevention, "Underlying Cause of Death 1999-2010," *CDC WONDER Database*. 2020.

[54] B. Xiao, Y. Xu, X. Bi, J. Zhang, and X. Ma, "Heart sounds classification using a novel 1-D convolutional neural network with extremely low parameter consumption," *Neurocomputing*, 2020.

[55] Z. Jiang and S. Choi, "A cardiac sound characteristic waveform method for in-home heart disorder monitoring with electric stethoscope," *Expert Syst. Appl.*, 2006.

[56] L. Jin and J. Dong, "Classification of normal and abnormal ECG records using lead convolutional neural

network and rule inference," *Sci. China Inf. Sci.*, 2017.

[57] P. Wang, J. Lu, B. Zhang, and Z. Tang, "A review on transfer learning for brain-computer interface classification," in *2015 5th International Conference on Information Science and Technology (ICIST)*, 2015, pp. 315–322.

[58] S. J. Pan and Q. Yang, "A survey on transfer learning," *IEEE Transactions on Knowledge and Data Engineering*. 2010.

[59] H. A. Abbass, J. Tang, R. Amin, M. Ellejmi, and S. Kirby, "Augmented cognition using real-time EEG-based adaptive strategies for air traffic control," in *Proceedings of the Human Factors and Ergonomics Society*, 2014.

[60] S. W. Min *et al.*, "Erratum to Acetylation of tau inhibits its degradation and contributes to tauopathy," *Neuron*. 2010.

[61] K. S. Hong and N. Naseer, "Reduction of delay in detecting initial dips from functional near-infrared spectroscopy signals using vector-based phase analysis," *Int. J. Neural Syst.*, 2016.

[62] F. Al-Shargie, T. B. Tang, and M. Kiguchi, "Assessment of mental stress effects on prefrontal cortical activities using canonical correlation analysis: an fNIRS-EEG study," *Biomed. Opt. Express*, vol. 8, no. 5, p. 2583, 2017.

[63] A. Curtin and H. Ayaz, "The Age of Neuroergonomics: Towards Ubiquitous and Continuous Measurement of Brain Function with fNIRS," *Jpn. Psychol. Res.*, 2018.

[64] W. Glannon, "Ethical issues with brain-computer interfaces," *Front. Syst. Neurosci.*, 2014.

[65] M. J. Khan, M. J. Hong, and K.-S. Hong, "Decoding of four movement directions using hybrid NIRS-EEG brain-computer interface," *Front. Hum. Neurosci.*, vol. 8, p. 244, 2014.

[66] B. Z. Allison, C. Brunner, V. Kaiser, G. R. Müller-Putz, C. Neuper, and G. Pfurtscheller, "Toward a hybrid brain-computer interface based on imagined movement and visual attention," *J. Neural Eng.*, 2010.

[67] G. Müller-Putz *et al.*, "Towards noninvasive hybrid brain-computer interfaces: Framework, practice, clinical application, and beyond," *Proc. IEEE*, 2015.

[68] H. O. Keles, R. L. Barbour, and A. Omurtag, "Hemodynamic correlates of spontaneous neural activity measured by human whole-head resting state EEG + fNIRS," *Neuroimage*, 2016.

[69] L. F. Nicolas-Alonso and J. Gomez-Gil, "Brain computer interfaces, a review," *Sensors*. 2012.

[70] M. A. Franceschini, D. K. Joseph, T. J. Huppert, S. G. Diamond, and D. A. Boas, "Diffuse optical imaging of the whole head," *J. Biomed. Opt.*, 2006.

[71] N. Naseer, N. K. Qureshi, F. M. Noori, and K. S. Hong, "Analysis of Different Classification Techniques for Two-Class Functional Near-Infrared Spectroscopy-Based Brain-Computer Interface," *Comput. Intell. Neurosci.*, 2016.

[72] A. Zafar and K. S. Hong, "Neuronal Activation Detection Using Vector Phase Analysis with Dual Threshold Circles: A Functional Near-Infrared Spectroscopy Study," *Int. J. Neural Syst.*, 2018.

[73] M. E. Spira and A. Hai, "Multi-electrode array technologies for neuroscience and cardiology," *Nature Nanotechnology*. 2013.

[74] S. D. Power, A. Kushki, and T. Chau, “Intersession consistency of single-trial classification of the prefrontal response to mental arithmetic and the no-control state by NIRS,” *PLoS One*, 2012.

[75] U. Asgher, R. Ahmad, N. Naseer, Y. Ayaz, M. J. Khan, and M. K. Amjad, “Assessment and Classification of Mental Workload in the Prefrontal Cortex (PFC) using Fixed-Value Modified Beer-Lambert Law,” *IEEE Access*, 2019.

[76] Y. Li *et al.*, “An EEG-based BCI system for 2-D cursor control by combining Mu/Beta rhythm and P300 potential,” *IEEE Trans. Biomed. Eng.*, 2010.

[77] F.-M. Lu and Z. Yuan, “PET/SPECT molecular imaging in clinical neuroscience: recent advances in the investigation of CNS diseases.,” *Quant. Imaging Med. Surg.*, 2015.

[78] N. Weiskopf *et al.*, “Principles of a brain-computer interface (BCI) based on real-time functional magnetic resonance imaging (fMRI),” *IEEE Trans. Biomed. Eng.*, 2004.

[79] J. D. Rieke *et al.*, “Development of a combined, sequential real-time fMRI and fNIRS neurofeedback system to enhance motor learning after stroke,” *J. Neurosci. Methods*, 2020.

[80] S. B. Borgheai *et al.*, “Enhancing Communication for People in Late-Stage ALS Using an fNIRS-Based BCI System,” *IEEE Trans. Neural Syst. Rehabil. Eng.*, 2020.

[81] J. B. F. Van Erp, F. Lotte, and M. Tangermann, “Brain-computer interfaces: Beyond medical applications,” *Computer (Long. Beach. Calif).*, 2012.

[82] R. Rao and R. Scherer, “Brain-Computer Interfacing [In the Spotlight,” *IEEE Signal Process. Mag.*, 2010.

[83] L. Bi, X.-A. Fan, and Y. Liu, “EEG-based brain-controlled mobile robots: a survey,” *IEEE Trans. human-machine Syst.*, vol. 43, no. 2, pp. 161–176, 2013.

[84] A. A. Navarro *et al.*, “Context-awareness as an enhancement of brain-computer interfaces,” in *Lecture Notes in Computer Science (including subseries Lecture Notes in Artificial Intelligence and Lecture Notes in Bioinformatics)*, 2011.

[85] K. S. Hong, M. J. Khan, and M. J. Hong, “Feature Extraction and Classification Methods for Hybrid fNIRS-EEG Brain-Computer Interfaces,” *Frontiers in Human Neuroscience*. 2018.

[86] U. Asgher *et al.*, “Enhanced Accuracy for Multiclass Mental Workload Detection Using Long Short-Term Memory for Brain–Computer Interface,” *Front. Neurosci.*, 2020.

[87] I. Chivers and J. Sleightholme, “An introduction to Algorithms and the Big O Notation,” in *Introduction to Programming with Fortran*, Springer, 2015, pp. 359–364.

[88] A. Tharwat, T. Gaber, A. Ibrahim, and A. E. Hassanien, “Linear discriminant analysis: A detailed tutorial,” *AI Commun.*, 2017.

[89] M. Sharir and M. H. Overmars, “A simple output-sensitive algorithm for hidden surface removal,” *ACM Trans. Graph.*, 1992.

[90] M. Taghavi and M. Shoaran, “Hardware complexity analysis of deep neural networks and decision tree ensembles for real-time neural data classification,” in *2019 9th International IEEE/EMBS Conference on Neural Engineering (NER)*, 2019, pp. 407–410.

[91] R. Pascanu, C. Gulcehre, K. Cho, and Y. Bengio, “How to construct deep recurrent neural networks,” in *2nd*

International Conference on Learning Representations, ICLR 2014 - Conference Track Proceedings, 2014.

[92] S. Zhang *et al.*, "Architectural complexity measures of recurrent neural networks," in *Advances in Neural Information Processing Systems*, 2016.

[93] U. Asgher, K. Khalil, Y. Ayaz, R. Ahmad, and M. J. Khan, "Classification of Mental Workload (MWL) using Support Vector Machines (SVM) and Convolutional Neural Networks (CNN)," in *2020 3rd International Conference on Computing, Mathematics and Engineering Technologies: Idea to Innovation for Building the Knowledge Economy, iCoMET 2020*, 2020.

[94] Y. Blokland *et al.*, "Combined EEG-fNIRS decoding of motor attempt and imagery for brain switch control: an offline study in patients with tetraplegia," *IEEE Trans. neural Syst. Rehabil. Eng.*, vol. 22, no. 2, pp. 222–229, 2014.

[95] C.-C. Lo, T.-Y. Chien, Y.-C. Chen, S.-H. Tsai, W.-C. Fang, and B.-S. Lin, "A wearable channel selection-based brain-computer interface for motor imagery detection," *Sensors*, vol. 16, no. 2, p. 213, 2016.

[96] K.-S. Hong and H. Santosa, "Decoding four different sound-categories in the auditory cortex using functional near-infrared spectroscopy," *Hear. Res.*, vol. 333, pp. 157–166, 2016.

[97] Z. Wu, Y. Lai, Y. Xia, D. Wu, and D. Yao, "Stimulator selection in SSVEP-based BCI," *Med. Eng. Phys.*, vol. 30, no. 8, pp. 1079–1088, 2008.

[98] A. Floriano, P. F Diez, and T. Freire Bastos-Filho, "Evaluating the influence of chromatic and luminance stimuli on SSVEPs from behind-the-ears and occipital areas," *Sensors*, vol. 18, no. 2, p. 615, 2018.

[99] P. F. Diez *et al.*, "Commanding a robotic wheelchair with a high-frequency steady-state visual evoked potential based brain--computer interface," *Med. Eng. Phys.*, vol. 35, no. 8, pp. 1155–1164, 2013.

[100] J. Li, J. Liang, Q. Zhao, J. Li, K. Hong, and L. Zhang, "Design of assistive wheelchair system directly steered by human thoughts," *Int. J. Neural Syst.*, vol. 23, no. 03, p. 1350013, 2013.

[101] C. S. Herrmann, "Human EEG responses to 1--100 Hz flicker: resonance phenomena in visual cortex and their potential correlation to cognitive phenomena," *Exp. brain Res.*, vol. 137, no. 3–4, pp. 346–353, 2001.

[102] A. Kuś Rafałand Duszyk *et al.*, "On the quantification of SSVEP frequency responses in human EEG in realistic BCI conditions," *PLoS One*, vol. 8, no. 10, p. e77536, 2013.

[103] G. R. Müller-Putz, R. Scherer, C. Brauneis, and G. Pfurtscheller, "Steady-state visual evoked potential (SSVEP)-based communication: impact of harmonic frequency components," *J. Neural Eng.*, vol. 2, no. 4, p. 123, 2005.

[104] R. Abiri, S. Borhani, E. W. Sellers, Y. Jiang, and X. Zhao, "A comprehensive review of EEG-based brain-computer interface paradigms," *J. Neural Eng.*, 2018.

[105] S. W. Brose *et al.*, "The role of assistive robotics in the lives of persons with disability," *Am. J. Phys. Med. Rehabil.*, vol. 89, no. 6, pp. 509–521, 2010.

[106] Á. Fernández-Rodr\'\iguez, F. Velasco-Álvarez, and R. Ron-Angevin, "Review of real brain-controlled wheelchairs," *J. Neural Eng.*, vol. 13, no. 6, p. 61001, 2016.

[107] A. Rezeika, M. Benda, P. Stawicki, F. Gembler, A. Saboor, and I. Volosyak, "Brain--computer interface spellers: A review," *Brain Sci.*, vol. 8, no. 4, p. 57, 2018.

[108] D. Zhang, B. Huang, W. Wu, and S. Li, “An idle-state detection algorithm for SSVEP-based brain--computer interfaces using a maximum evoked response spatial filter,” *Int. J. Neural Syst.*, vol. 25, no. 07, p. 1550030, 2015.

[109] E. Galy, M. Cariou, and C. Mélan, “What is the relationship between mental workload factors and cognitive load types?,” *Int. J. Psychophysiol.*, 2012.

[110] R. Hosseini, B. Walsh, F. Tian, and S. Wang, “An fNIRS-Based Feature Learning and Classification Framework to Distinguish Hemodynamic Patterns in Children Who Stutter,” *IEEE Trans. Neural Syst. Rehabil. Eng.*, 2018.

[111] C. Herff, D. Heger, F. Putze, J. Hennrich, O. Fortmann, and T. Schultz, “Classification of mental tasks in the prefrontal cortex using fNIRS,” in *Proceedings of the Annual International Conference of the IEEE Engineering in Medicine and Biology Society, EMBS*, 2013.

[112] L. C. Schudlo and T. Chau, “Dynamic topographical pattern classification of multichannel prefrontal NIRS signals: II. Online differentiation of mental arithmetic and rest,” *J. Neural Eng.*, 2014.

[113] M. V. Kosti, K. Georgiadis, D. A. Adamos, N. Laskaris, D. Spinellis, and L. Angelis, “Towards an affordable brain computer interface for the assessment of programmers’ mental workload,” *Int. J. Hum. Comput. Stud.*, 2018.

[114] D. J. McFarland, W. A. Sarnacki, and J. R. Wolpaw, “Brain-computer interface (BCI) operation: Optimizing information transfer rates,” *Biol. Psychol.*, 2003.

[115] B. Obermaier, C. Neuper, C. Guger, and G. Pfurtscheller, “Information transfer rate in a five-classes brain-computer interface,” *IEEE Trans. Neural Syst. Rehabil. Eng.*, 2001.

[116] N. Naseer and K. S. Hong, “Classification of functional near-infrared spectroscopy signals corresponding to the right- and left-wrist motor imagery for development of a brain-computer interface,” *Neurosci. Lett.*, 2013.

[117] Thesis title: "Fixed-Value MBLL Based Cognitive Hemodynamic Response Assessment Using PfNIRS System: Application to Deep Learning Brain Machine Interface. By Umer Asgher. Thesis date 21 September 2020. SMME- National University of Sciences and Technology (NUST), Islamabad, Pakistan.